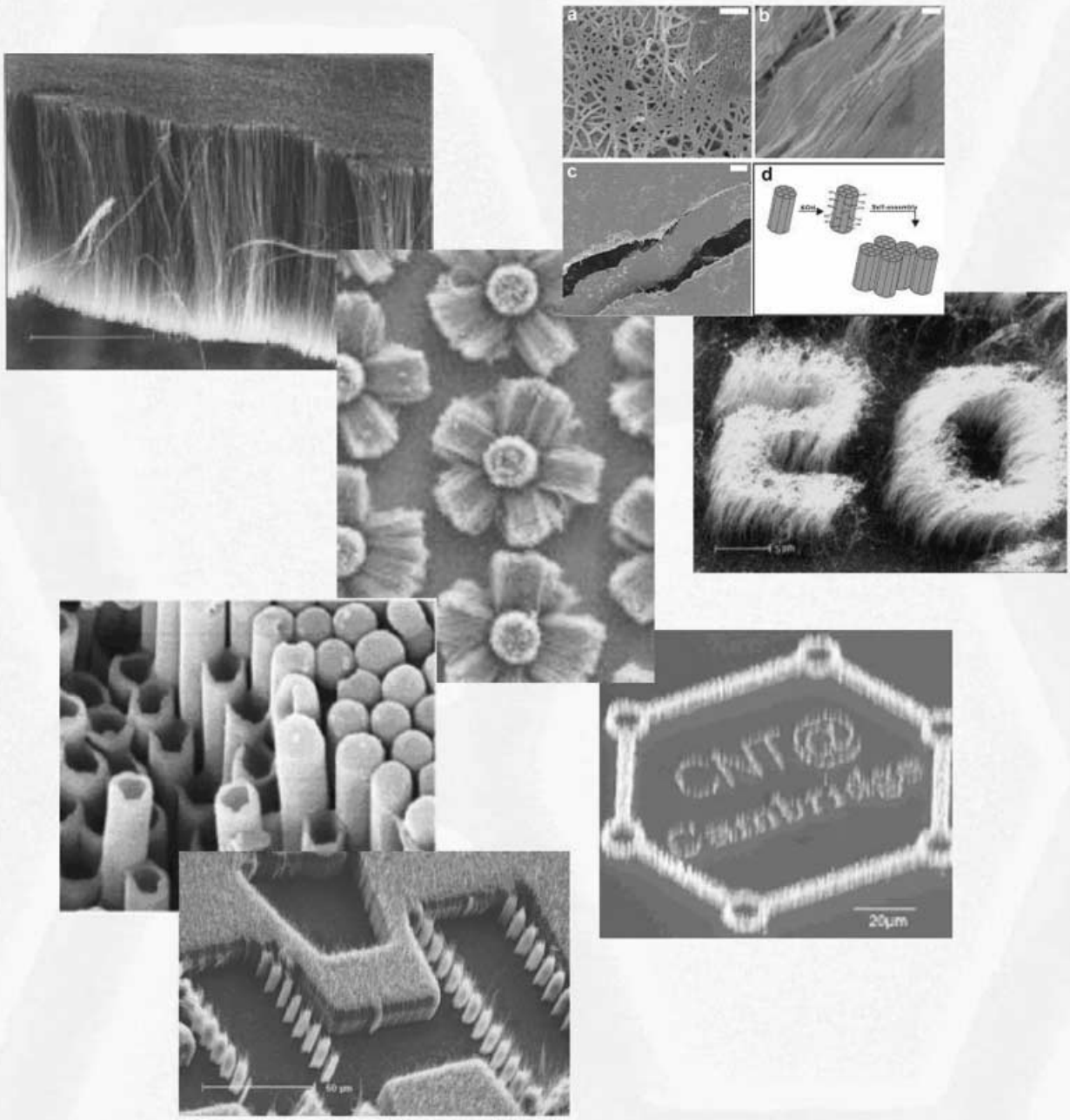

Nanotubes have been shown to exhibit superior properties attractive for various potential applications, ranging from their use as novel electron emitters in flat panel displays to electrodes in electrochemical sensors. For many of the applications, it is highly desirable to have aligned/patterned forms of carbon nanotubes so that their structure/property can be easily assessed while they can be effectively incorporated into devices. Judicious application of various micro-/nanofabrication techniques has led to the development of many sophisticated structures of aligned nanotubes of practical significance. The above images show recent progresses in the synthesis and micro-/nanofabrication of aligned carbon and noncarbon nanotubes.

  DOI: 10.1002/cphc.200300770

Aligned Nanotubes

Liming Dai,*[a] Ajeeta Patil,[a] Xiaoyi Gong,[b] Zhixin Guo,*[c] Luqi Liu,[c] Yong Liu,[c] and Daoben Zhu[c]

Since the discovery of carbon nanotubes by Iijima in 1991, various carbon nanotubes with either a single- or multilayered graphene cylinder(s) have been produced, along with their noncarbon counterparts (for example, inorganic and polymer nanotubes). These nanostructured materials often possess size-dependent properties and show new phenomena related to the nanosize confinement of the charge carriers inside, which leads to the possibility of developing new materials with useful properties and advanced devices with desirable features for a wide range of applications. In particular, carbon nanotubes have been shown to exhibit superior properties attractive for various potential applications, ranging from their use as novel electron emitters in flat-panel displays to electrodes in electrochemical sensors. For many of the applications, it is highly desirable to have aligned/patterned forms of carbon nanotubes so that their structure/property can be easily assessed and so that they can be effectively incorporated into devices. In this Review, we present an overview on the development of aligned and micropatterned nanotubes, with an emphasis on carbon nanotubes.

1. Introduction

1.1. What are Nanotubes?

Nanotechnology is the creation of useful materials, devices, and systems through the control of matter on the nanometer scale and the exploitation of novel properties and phenomena developed at that length scale.[1] At the nanometer scale, the wavelike properties of electrons inside matter and atomic interactions are influenced by the size of the material.[2] As a consequence, changes in melting points, magnetic, optical, and/or electronic properties can be observed as the material takes on nanoscale dimensions.[2] Due to the high surface-to-volume ratio associated with nanometer-sized materials, a tremendous improvement in chemical properties is also achievable through the reduction in size.[2] Besides, new phenomena, such as the confinement-induced quantization effect, also occur when the size of materials becomes comparable to the de Broglie wavelength of the charge carriers inside.[2] By creating nanostructures, therefore, it is possible to control the fundamental properties of materials even without changing the materials' chemical composition. This should, in principle, allow us to develop a large number of new materials and devices of desirable properties and useful functions for numerous applications.

Indeed, the recent discovery of carbon nanotubes by Iijima[3] in 1991 opened up a new era in material science and nanotechnology. Since then, various carbon nanotubes with either a single- or multilayered graphene cylinder(s), along with their noncarbon counterparts, have been produced by arc-discharge, chemical vapor deposition (CVD), or laser ablation.[4–6] As can be seen in Figure 1, carbon nanotubes may be viewed as a graphite sheet that is rolled up into a nanoscale tube form (single-walled carbon nanotubes, SWNTs) or with additional graphene tubes around the core of a SWNT (multiwalled carbon nanotubes, MWNTs).[4–6]

These elongated nanotubes consist of carbon hexagons arranged in a concentric manner, with both ends of the tubes normally capped by fullerene-like structures containing pentagons. They usually have a diameter ranging from a few Ångstroms to tens of nanometers, and a length of up to several centimeters. Because the graphene sheet can be rolled up with varying degrees of twist along its length, carbon nanotubes have a variety of chiral structures.[4–6] Depending on their diameter and the helicity of the arrangement of graphite rings, carbon nanotubes can exhibit semiconducting or metallic behavior. Dissimilar carbon nanotubes may even be joined together to form molecular wires with interesting electronic, magnetic, nonlinear optical, and mechanical properties.[4–9] Soon after the discovery of the carbon nanotube, it became clear that similar nanoscale tubular structures could also be formed by various noncarbon materials, including alloyed carbon nanotubes (for

[a] *Prof. L. Dai, A. Patil*
Department of Polymer Engineering
College of Polymer Science and Polymer Engineering
The University of Akron, Akron, OH44325-0301 (USA)
Fax: (+1) 330 – 258 – 2339
E-mail: ldai@uakron.edu

[b] *Dr. X. Gong*
Conoco, Inc., P.O. Box 1267, 1000 South Pine
Ponca City, OK 74602-1267 (USA)

[c] *Prof. Z. Guo, Dr. L. Liu, Y. Liu, Prof. D. Zhu*
Center for Molecular Science and Laboratory of Organic Solids
Institute of Chemistry, Chinese Academy of Sciences
Beijing 100080 (China)
Fax: (+86) 10 – 6255 – 9397
E-mail: gzhixin@iccas.ac.cn

 DOI: 10.1002/cphc.200300770

example, BN, $B_xC_yN_z$, GaP, GaAs), oxide nanotubes (for example, SiO_2, Al_2O_3, V_2O_5, TiO_2), and polymer nanotubes (for example, polyacrylonitrile, polyaniline, peptide).[10] Owing to their great diversity, noncarbon nanotubes can exhibit a wide range of different properties.[10] Unlike carbon nanotubes, for example, the bandgap of all BN nanotubes does not change with their radius, helicity, and interwall interactions, due to the ionic origin of the large bandgap.[11, 12] These interesting properties allow carbon nanotubes and their noncarbon counterparts to be useful for many potential applications, for example, as new materials for the development of novel single-molecular transistors,[13–15] scanning probe microscope tips,[16–19] molecular computing elements,[20] electron-field-emitting flat-panel displays,[21–26] gas and electrochemical storage,[27–32] molecular-filtration membranes,[33] artificial muscles,[34] and sensors.[35] For most of the applications, however, an aligned/patterned form of carbon nanotubes is highly desirable.

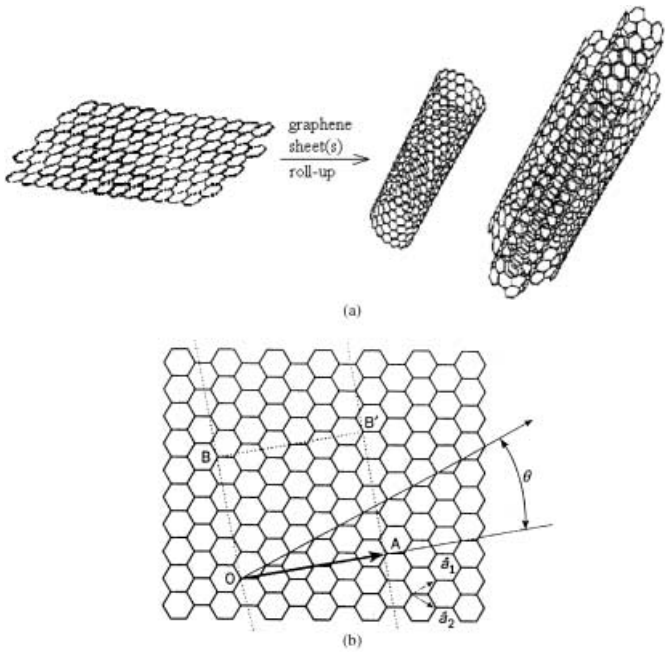

Figure 1. *Schematic representation of a) single-/multi-walled carbon nanotube formation by rolling up graphene sheet(s) and b) carbon nanotube formation based on a 2D graphene sheet of lattice vectors* a_1 *and* a_2*, the roll-up chiral vector* $C_h = na_1 + ma_2$*, and the chiral angle* θ *between* C_h *and* a_1*. When the graphene sheet is rolled up to form the cylindrical part of the nanotube, the chiral vector forms the circumference of nanotube's circular cross-section with its ends meeting each other. The chiral vector* (n,m) *defines the tube helicity.*

Liming Dai received his B.Sc. from Zhejiang University in 1983. He completed his Ph.D. at the Australian National University in 1990. He was a postdoctoral Fellow in the Cavendish Laboratory at Cambridge University from 1990 to 1992 and a visiting research faculty member in the University of Illinois at Urbana-Champaign in 1992. Thereafter, he had worked in the CSIRO Molecular Science in Melbourne for ten years before he returned to the United States in early 2002. He is currently an Associate Professor of Polymer Engineering at The University of Akron, where his group works on the synthesis and micro-/nanofabrication of functional polymers and carbon nanomaterials. He is also an Editorial Board Member for the Journal of Nanoscience and Nanotechnology and a Regional Receiving Editor for the *Australian Journal of Chemistry – An International Journal of Chemical Science.*

Zhi-Xin Guo, born in 1967, received his B.Sc. in Chemistry from Fudan University (Shanghai, 1988), M.Sc. in Organic Chemistry from Northwest University (Xi,an, 1991), and Ph.D. in Physical Chemistry from Tsinghua University (Beijing, 1996). Following postdoctoral studies in Chinese Academy of Sciences (Beijing, China) and Clemson University (USA), he joined the Institute of Chemistry, Chinese Academy of Sciences (Beijng, 2000) as a Research Professor. His interests include carbon nanotubes, fullerenes, and other organic functional materials.

1.2. The Necessity for Aligned and Micropatterned Carbon Nanotubes

1.2.1. Molecular Computing

During the last several decades, there has been tremendous progress in the field of electronics and computers. The need for cheaper, faster, and more accurate calculations has been a driving force for the development of even smaller computing devices, in which molecular electronics play a vital role. The recent advances in nanoscience and nanotechnology have made it possible to build single-molecule switches and memory elements. They can perform functions analogous to some key components of microcircuits, such as diodes and transistors. In this context, carbon nanotubes have been used both as active components and as molecular wires in molecular-scale electronics. At the molecular scale, how to connect wires to device components (for example, molecular transistors or diodes) has been one of the long-standing problems, and still remains a big challenge.

To address the above problem, Lieber and co-workers[20] have recently devised a crisscrossed carbon nanotube relay consisting of a set of parallel SWNTs on a substrate and a set of perpendicular SWNTs suspended over a parallel nanotube array (Figure 2).

As shown in Figure 2, each cross point in the crisscrossing nanotube array corresponds to a device element with a switch ON (a contact upper-to-lower nanotube junction with a low resistance) and OFF (a separated upper-to-lower nanotube

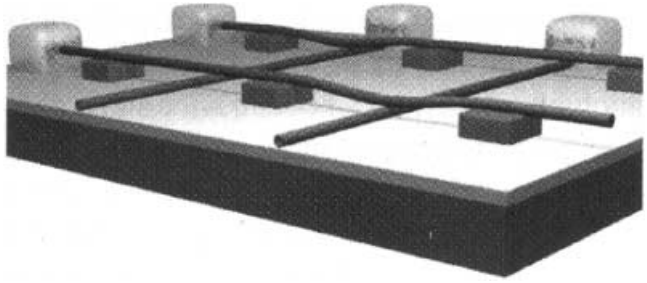

Figure 2. *3D view of a suspended cross-bar array of carbon nanotubes of four junctions, showing two elements in the ON (contact) state and two elements in the OFF (separated) state. The substrate is made of a highly doped silicon conducting layer (dark gray) coated with a thin dielectric SiO_2 layer (light gray). While the lower nanotubes lie down directly on the dielectric film, the upper nanotubes are suspended on a periodic array of nonconducting inorganic or organic supports (gray blocks).*[20]

junction with a high resistance) state. A device element could be switched between these well-defined ON and OFF states by applying a certain voltage with alternatively changing bias to the two nanotubes. Theoretical calculations have demonstrated that these reversible and bistable nanotube device elements could be used to construct nonvolatile random access memory (RAM) and logic function tables.[20] Owing to their tiny size, and the good electrical and mechanical properties intrinsically characteristic of SWNTs, an integration level approaching 10^{12} elements per square centimeter and an element operation frequency in excess of 100 GHz are achievable.

1.2.2. Field Emission

Carbon nanotubes have also been explored for use as new electron field emitters in panel displays.[21–26] The carbon-nanotube electron emitters work on a similar principle to a conventional cathode ray tube, but their small size could lead to a thinner, more flexible, and energy efficient display screen with a higher resolution. The field emission study on single-wall carbon nanotubes carried out by de Heer and co-workers[36] showed some promising results with a turn-on field, E_{to} (defined as the electric field required to emit a current $I = 10\ \mu A\,cm^{-2}$), in the range of 1.5 – 4.5 V/μm and a threshold field, E_{thr}, (that is, the electrical field corresponding to $I = 10\ mA\,cm^{-2}$) in the range of 3.9 – 7.8 V/μm. These values, like those for most MWNTs, are far lower than corresponding values for other film emitters. Field emissions from an epoxy-carbon nanotube composite have also been reported.[32] More interestingly, Saito et al.[37, 38] have constructed an electron-tube lighting element equipped with MWNT field emitters as the cathode. In this study, stable electron emission, bright luminance, and a long life suitable for various practical applications have been demonstrated. More recently, some prototype carbon-nanotube field-emission displays have been reported.[39–46] Although aligned carbon nanotubes are not necessary for these display applications, the use of aligned/micropatterned carbon nanotubes has been shown to offer additional advantages for the development of low field nanotube-based flat-panel displays.[47]

1.2.3. Membrane Applications

The use of the hollow, aligned carbon-nanotube films as a fast and energy-efficient means for water desalination has also been proposed.[33, 48, 49] In particular, the vertically aligned carbon nanotube films with opened nanotube tips are electrically charged so that sodium and chloride ions are electrostatically adsorbed onto the tube surface when salt-water runs through the nanotube hollow core. The electrostatically adsorbed ions can be released into a waste stream by rapidly removing the charge. Due to the high electrical conductivity and large surface area, the aligned carbon-nanotube films are far more efficient than ordinary carbon for removing the salt from water.

The above examples clearly illustrate that aligned and/or micropatterned structures are critical for the use of nanotubes in many applications of practical significance. Therefore, research on the synthesis of aligned nanotubes and their microfabrication has received ever-increasing attention. Recent developments in the field have indicated that the use of various advanced synthetic and micropatterning techniques could lead to a wide range of ordered (for example, both horizontally and perpendicularly aligned/micropatterned) nanotubes of much improved properties, and nanodevices of novel features. This review is meant to provide readers with a status summary of recent developments in the synthesis and micropatterning of aligned carbon and noncarbon nanotubes. In what follows, we will first present an overview of the various methods for preparing *horizontally* aligned and micropatterned carbon nanotubes. We will then highlight some pyrolytic methods for the growth of *perpendicularly* aligned and micropatterned carbon nanotubes. This will be followed by a demonstration of several *self-assembling* approaches towards the synthesis of vertically aligned carbon nanotubes. The synthesis and microfabrication of aligned, noncarbon nanotubes will then be discussed with some examples.

2. Horizontally Aligned and Micropatterned Carbon Nanotubes

2.1. Horizontally Aligned Carbon Nanotubes

As can be seen from the above discussion, the arrays of carbon nanotubes are useful for molecular computing.[20] Horizontally aligned carbon nanotubes have been prepared either by slicing a nanotube-dispersed polymer composite or by rubbing a nanotube-deposited plastic surface with a thin sheet of Teflon or aluminum foil.[21, 50] In 1994, Ajayan[51] developed a simple technique for producing aligned arrays of carbon nanotubes. He mixed the nanotubes with epoxy-based resin. The nanotube-resin mixture was hardened and then cut into slices ranging in thickness from 50 to 1000 nm with lateral dimensions of a few millimeters. Transmission electron microscopy (TEM) images of the slices show that the tubes were preferentially oriented parallel during the cutting process (Figure 3). His results demonstrated the nature of rheology, on a nanometer scale, in composite media and flow-induced anisotropy produced by the

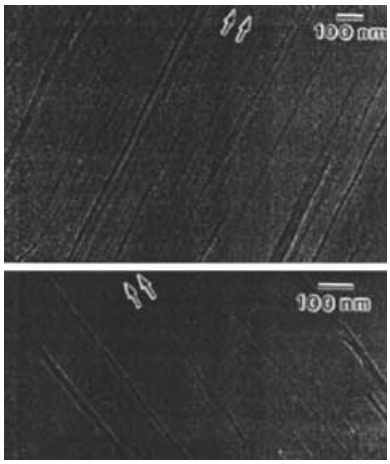

Figure 3. *TEM image of aligned carbon nanotube arrays in a thin film of polymer expoxy obtained by cutting the nanotube/polymer composite.[51]*

cutting process, and also suggested the excellent mechanical properties of carbon nanotubes.

On the other hand, de Heer et al.[21] produced nanotube thin films by a filtering-pressing method. The tubes can be aligned either parallel or perpendicular to the surface of the films by drawing the tube suspension through a 0.2 μm-pore ceramic filter, which left a uniform black deposit on the filter. The parallely aligned surfaces are birefringent, reflecting differences in the dielectric function along, and normal to, the tubes. Recently, Kroto and co-workers[52] reported a method for aligning carbon nanotubes by the pyrolysis of 2-amino-4,6-dichloro-*s*-triazine on a silica substrate prepatterned with a cobalt catalyst by laser ablation.

More recently, Guo and co-workers[53] have developed a new approach for modifying carbon nanotubes with multiple hydroxy groups (designated as carbon nanotubols) via a simple solid-phase mechanochemical reaction with potassium hydroxide at room temperature. The carbon nanotubols thus produced are highly soluble in water and can readily self-assemble into aligned arrays upon drying.

As shown in Figure 4, the scanning electron microscopy (SEM) image for the starting buckypaper made from an SWNT suspension of Tube@Rice (Figure 4a) shows a randomly entangled morphology. In contrast, the cross-section SEM image of a centrifuged nanotubol film, prepared by ball-milling a piece of buckypaper in the presence of KOH,[53] revealed self-assembled arrays with a well-aligned structure (Figure 4b). Figure 4c indicates the occurrence of a large-scale self-assembling process. As schematically illustrated in Figure 4d, the strong hydrogen-bonding interaction between the nanotubols is believed to be the driving force for the formation of the highly oriented, self-assembled nanotubol arrays.

2.2. Micropatterning of Nonaligned and Horizontally Aligned Carbon Nanotubes

Burghard et al.[54] have reported the region-specific deposition of carbon nanotubes grafted with surfactants containing negatively charged groups (for example, sodium dodecylsulfate) onto

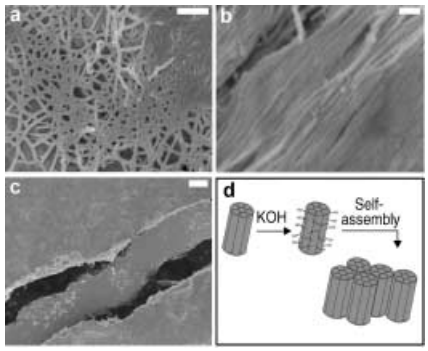

Figure 4. *SEM images of a) the starting SWNT sample (scale bar, 100 nm); b) cross-sectional view of the self-assembled SWNT nanotubols sample shown in (c) (scale bar, 100 nm); c) Top view of the self-assembled SWNT nanotubol sample (scale bar, 1000 nm); and d) A schematic representation of the self-assembling process.[53]*

substrate surfaces prepatterned with positively charged functionalities (for example, ammonium groups on silanized silica). Subsequently, Liu et al.[55] demonstrated that individual single-wall carbon nanotubes purified by refluxing in HNO_3 (2.6 M) could be region-specifically deposited onto surfaces prepatterned with a self-assembled monolayer (SAM) of $-NH_2$ functionalities. In a separate study, we have developed a versatile method for making patterns of nonaligned carbon nanotubes.[56] In particular, we first generated plasma-induced (either by nondepositing plasma treatment or by plasma polymerization) surface patterns of $-NH_2$ groups onto a substrate (for example, a quartz glass plate, mica sheet, or polymer film), and then performed region-specific adsorption of the COOH-containing carbon nanotubes from an aqueous medium, through the polar–polar interaction between the COOH groups and the plasma-patterned $-NH_2$ groups. The COOH-containing carbon nanotubes were prepared by the acid treatment (HNO_3)[57] of the nanotubes generated by pyrolysis of iron(II) phthalocyanine ($FeC_{32}N_8H_{16}$, designated as FePc).[58] Figure 5 reproduces a SEM image of the

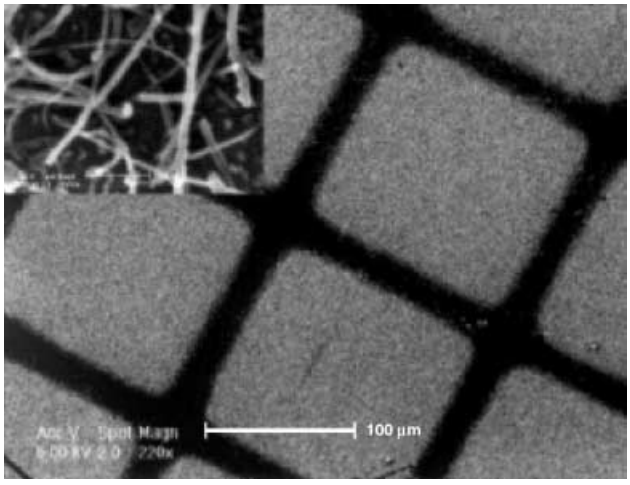

Figure 5. *SEM images of adsorbed COOH-containing carbon nanotubes (within the squared areas) on a heptylamine-plasma patterned mica sheet. Inset gives a higher magnification image of the plasma covered areas, showing the individual adsorbed carbon nanotubes.[56]*

COOH-containing carbon nanotubes region-specifically adsorbed (about 2.5 mg/10 mL H_2O) onto a mica sheet prepatterned with the heptylamine-plasma polymer (200 kHz, 10 W, and a monomer pressure of 0.13 torr for 30 s). The adsorbed carbon nanotubes are clearly evident by inspection of the plasma-patterned areas of Figure 5 under a higher magnification (inset of Figure 5). The corresponding high-magnification SEM image for the plasma-polymer-free areas revealed an almost featureless smooth surface characteristic of a mica sheet. No adsorption of the carbon nanotubes was observed in a control experiment when a pure mica sheet was used as the substrate.

More recently, Zhou and co-workers[59] have demonstrated the preparation of ordered/micropatterned carbon nanotubes through the self-assembly of preformed carbon nanotubes on glass, and certain other substrates, by vertically immersing the substrate into an aqueous solution of acid-oxidized short SWNTs.[57] Figure 6a schematically shows the self-assembly process. No carbon nanotube deposition was observed for a hydrophobic substrate (for example, a polystyrene spin-coated glass slide) under the same conditions. This selectivity enabled the fabrication of carbon nanotube patterns by using glass substrates with prepatterned hydrophobic and hydrophilic regions. Figure 6b shows optical microscopic images for some of the SWNT micropatterns thus prepared.

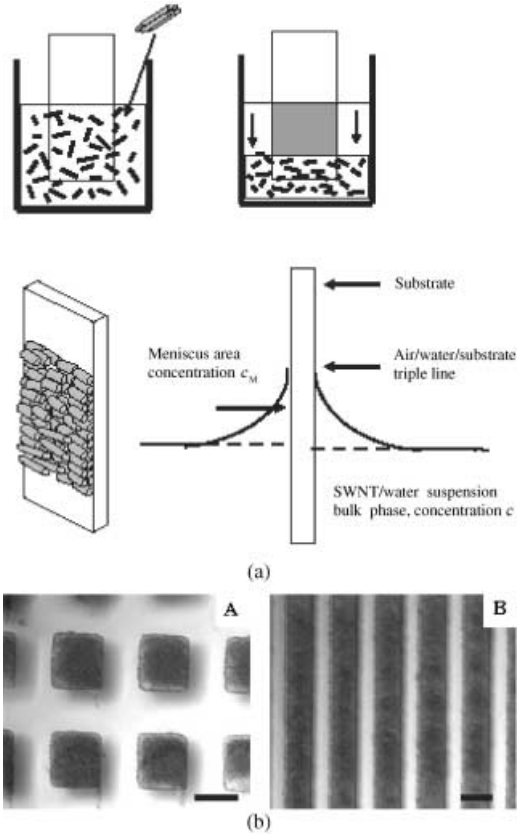

Figure 6. *a) A schematic representation of the self-assembly process. A hydrophilic glass slide was vertically immersed into an aqueous solution of acid-oxidized SWNTs, followed by gradual evaporation of the water at room temperature. The SWNT bundles self-assembled on the glass substrate around the air/water/substrate interface. As the interface progressed downwards, a continuous SWNT film was formed on the glass substrate. b) Patterned SWNT structures formed by the self-assembly process on hydrophobic substrates prepatterned with periodic hydrophilic regions: A) the squares are 100 μm × 100 μm, and B) the strips are 100 μm wide. The shadows are due to reflections from the surface on which the samples were placed. The scale bars in both (A) and (B) are 100 μm.*[59]

Just as microchips have revolutionized computers and electronics, the micro-/nanopatterned carbon nanotubes described above could have the potential to revolutionize many industrial sectors. In order to construct and operate new devices at the nanometer scale, however, the proper connection from nanoscale entities to the macroscale world still remains a big challenge. In this context, Dai and co-workers[60] at Stanford have demonstrated the ability to grow SWNT wires between controlled surface sites by catalyst patterning, leading to a variety of interconnecting SWNT architectures, which includes a suspended SWNT power line and a square of suspended SWNT bridges (Figure 7).

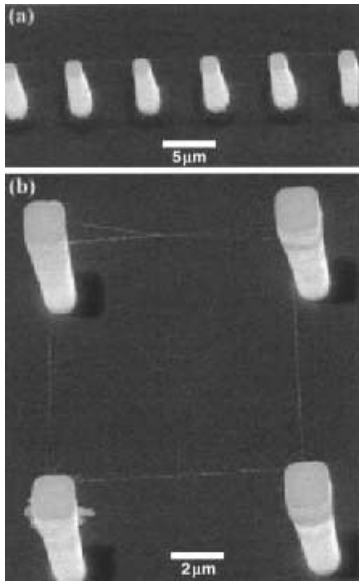

Figure 7. *SEM images of a) a suspended SWNT power line and b) a square of suspended SWNT bridges.*[60]

In so doing, these authors developed a liquid-phase catalyst precursor, which was patterned onto silicon towers using the contact printing (μcp) technique. Calcination of the silica-tower-supported catalyst, followed by the CVD growth of SWNTs, resulted in the formation of a SWNT network between adjacent towers. More recently, Joselevich and Lieber[61] have demonstrated a new approach to vectorial growth of SWNT arrays by patterning the catalyst nanoparticles and applying a local electric field parallel to the substrate. These SWNT network can be utilized as power lines to address nanoscale components in nanodevices. By controlling the arrangement of silicon towers, the growth of the suspended SWNTs can be directed to create the desired architecture.

In a closely related, but independent work, Ajayan and co-workers[62] attempted to synthesize MWNTs on the surface of magnesium oxide cubes in order to enhance the possibility of creating networks over which nanotubes can be distributed.

MgO cubes can be treated as the distribution sites. The MgO cube templates were prepared by burning Mg ribbons in ambient air and depositing the smoke on clean, planar Si wafers. The MgO cubes thus prepared possess a good reaction site density, and thus are considered apt as a substrate for the deposition of carbon nanotubes by CVD. It has been demonstrated that different facets of the cubes have different densities and growth rates for the nanotube formation. Parameters such as the orientation of MgO cubes and the flow direction of the catalyst feed stream govern the growth and orientation of the nanotubes. Thus, the synthesis of carbon nanotubes on the MgO surface could help to build up networks, which can be used to transport electrical signals by developing an interface between the templates and nanotube structure.

Besides, similar liquid-phase catalyst precursor approaches have also been used to prepare perpendicularly aligned carbon nanotubes by predepositing catalytic metal species onto a substrate surface with certain liquid carries, followed by the pyrolysis of appropriate hydrocarbon vapor(s).[63]

3. Perpendicularly Aligned and Micropatterned Carbon Nanotubes

As can be seen from the above discussion, various techniques have been developed for the preparation of *horizontally* aligned and micropatterned carbon nanotubes of practical significance. Carbon nanotubes aligned *perpendicular* to a substrate offer additional advantages for many applications, including their use as electron emitters and molecular membranes.

3.1. Template-Synthesis and Fabrication of Perpendicularly Aligned Carbon Nanotubes

In order to construct a nanotube field emitter, de Heer et al.[21] first made an ethanol dispersion of arc-produced carbon nanotubes, which was then passed through an aluminum oxide micropore filter to align nanotubes perpendicularly onto the filter surface. These authors then transferred the perpendicularly aligned carbon nanotubes onto a cathode substrate in a field-emitting device for electron emission measurements. The internanotube sticking interaction and the inhomogeneity in tube length were found to affect the emission performance. They also measured the optical properties of these highly ordered and densely packed nanotubes. The perpendicularly aligned carbon nanotubes showed different dielectric behavior in the directions parallel and at 90° to the tubes.

Using a similar porous membrane (for example, mesoporous silica, alumina nanoholes), the so-called template synthesis technique has been used to prepare aligned carbon nanotubes.[64, 65] In this regard, Xie and co-workers[66] were the first to report the large-scale CVD growth of aligned carbon nanotubes from a mesoporpous silica template with embedded iron nanoparticles. The nanotubes' direction of growth can be controlled by the orientation of the pores from which the nanotubes grow. Similarly, Xu and co-workers[67] have reported the controlled growth of aligned carbon nanotubes by the pyrolysis of hydrocarbon on a nickel catalyst embedded in a porous silicon substrate. In these cases, porous silicons containing micro-, meso-, and macropores were produced by electrochemically etching the crystalline silicon wafer (as the anode) in an aqueous HF solution (using a Pt wire as the cathode). Generally speaking, anodic aluminum oxide films can be used for producing aligned carbon nanotubes with uniform diameters and lengths by the pyrolysis of organic molecules into the well-defined nanopores either with or without a catalyst.[68, 69]

More recently, Li et al.[70] have produced Y-shaped carbon nanotubes by the pyrolysis of methane over cobalt-covered magnesium oxide[71] using branched nanochannel alumina templates (Figure 8).

In this case, these authors first prepared the template with Y-branched nanochannels by anodizing a highly pure aluminum sheet in 0.3 M oxalic acid at 10°C under a constant voltage of 50 V

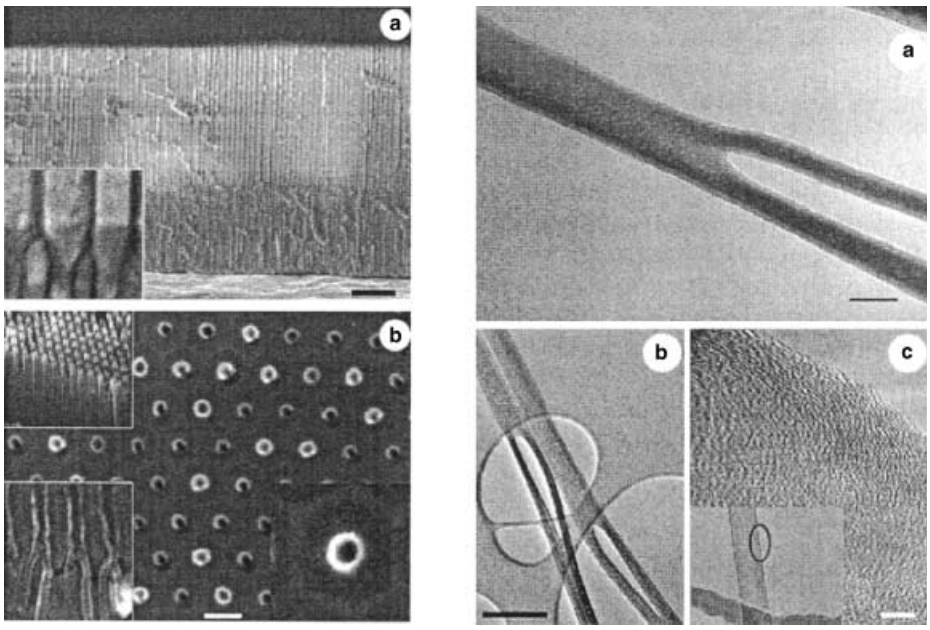

Figure 8. *Left: a) SEM image of a Y-branched nanochannel template (scale bar, 1 μm). The inset shows where the Y branches start to grow. b) Top-view SEM image of carbon nanotubes aligned in the template after ion-milling of amorphous carbon on the surface (scale bar, 100 nm). The nanotube diameter is larger than the original pore owing to thermal expansion of the template during growth. Top inset, stem part of the Y-junction tubes. Bottom left inset, close-up of the region between stem and branch portions still embedded in the template. Bottom right inset, close-up of the top of the nanotube in its hexagonal cell. Right: TEM image of a) the Y-junction tube (scale bar, 50 nm) with a stem of about 90 nm and branches 50 nm in diameter. b) Y-junction formed by using higher anodization voltages, resulting in stems of about 100 nm and branches 60 nm in diameter (scale bar, 200 nm). c) High-resolution TEM image of a typical Y-junction nanotube wall showing graphitic multiwall structure (scale bar, 5 nm). Inset shows the part of the tube that was imaged.*[69]

for 15 h, which resulted in an hexagonal array of pores near the aluminum surface. After chemically removing the original film, a second anodization was performed under the same conditions, typically for 30 min. The anodization voltage was then reduced to about 35 V. Because the pore cell diameter is proportional to the anodization voltage, reducing the voltage by a factor of $1/\sqrt{2}$ resulted in twice as many pores appearing in order to maintain the original total area of the template, and nearly all the pores branched into two, smaller-diameter pores. As a consequence, the resulting template consisted of parallel Y-branched pores with stems about 90 nm in diameter and branches about 50 nm in diameter.

3.2. Template-Free Synthesis of Aligned Carbon Nanotubes

Without using template pores, Rao et al.[72] have also successfully prepared aligned carbon nanotube arrays by the pyrolysis of ferrocene at about 900°C on a pristine quartz substrate. The same ferrocene molecule provides both the metal catalyst and the carbon source required for nanotube growth. In a separate study, Ren et al.[73] synthesized large arrays of well-aligned carbon nanotubes by radio-frequency sputter-coating a thin nickel layer onto display glass, followed by plasma-enhanced hot filament CVD of acetylene in the presence of ammonia gas below 666°C. Using similar conditions, these authors have also prepared highly aligned MWNTs on polished polycrystalline and single crystal nickel substrates.[74] Many parameters, including the plasma intensity, the acetylene to ammonia gas ratio, and their flow rates were found to affect the diameter and uniformity of the aligned carbon nanotubes. So far, various plasma techniques, including direct-current,[75, 76] radiofrequency,[77] and microwave plasmas,[78–81] have been used to enhance the production of aligned carbon nanotubes. On the other hand, Avigal and Kalish[82] prepared aligned carbon nanotubes by the pyrolysis of methane/argon onto Co-covered Si at 800°C in a regular cold-wall CVD reactor under an electric field. Kamalakaran et al.[83] reported the production of aligned carbon nanotube arrays by the pyrolysis of a jet solution of ferrocene and benzene in an argon atmosphere at relatively low temperatures (850°C).

We, along with others,[72, 84–87] have prepared large-scale, carbon nanotubes aligned perpendicular to the substrate surface by the pyrolysis of FePc under Ar/H_2 at 800 – 1100°C.[58] Figure 9 shows that the constituent carbon nanotubes have fairly uniform lengths and diameters. As demonstrated elsewhere,[88] the constituent straight nanotubes have a well-graphitized (graphite-like) multiwall structure with an outer diameter in the range of 35 – 55 nm.

Like the process reported by Rao et al.,[72] the use of organic-metal complexes containing both a metal catalyst and a carbon source (for example, ferrocene, FePc) for producing aligned carbon nanotubes is of particular interest. This one-step nanotube growth process requires no pretreatment of the substrate surface and could significantly facilitate the formation of aligned nanotube patterns for device applications, as we shall see later.

Figure 9. *A typical SEM image of the aligned carbon nanotube film prepared by pyrolysis of FePc. The misalignment seen for some of the nanotubes at the edge was caused by the peeling action used in the SEM sample preparation.*[58]

3.3. Perpendicularly Aligned Carbon Nanotubes by Self-Assembly

Compared to the large number of publications on the (perpendicular) alignment of carbon nanotubes discussed above, the *post-synthesis* ordering of chemically and/or physically modified carbon nanotubes is much less discussed in the literature. Nevertheless, perpendicularly aligned carbon nanotubes have been constructed from some end-functionalized carbon nanotubes on certain pretreated substrates, though these approaches deserve further investigation. For instance, Liu et al.[89] have prepared aligned SWNTs by self-assembling nanotubes end-functionalized with thiol groups on a gold substrate (Figure 10).

As seen in Figure 10, the carboxy-terminated short SWNTs prepared by acid oxidation were used as the starting material for further functionalization with thiol-containing alkyl amines through the amide linkage. Then, the self-assembly of aligned SWNTs was obtained by dipping a gold (111) ball into the thiol-functionalized SWNT suspension in ethanol, followed by ultrasonication and drying in high-purity nitrogen. The resulting self-assembled aligned nanotube film was so stable that ultrasonication could not remove it from the gold substrate. The packing density of the self-assembled, aligned carbon nanotubes was found to depend strongly on the incubation time.

As seen in the atomic force microscopy (AFM) images given in Figure 11, a shorter nanotube assembly with a lower packing density was formed with a shorter adsorption time, whereas a longer adsorption time resulted in the formation of an aligned nanotube array with a longer length and a higher packing density.

Given that carboxylic acids could be deprotonated by various metal oxides (for example, Ag, Al, Cu), Liu and co-workers[90] have also investigated the formation of perpendicularly aligned nanotube arrays by self-assembling COOH-terminated carbon nanotubes onto certain metal oxide substrates (for example, Ag).

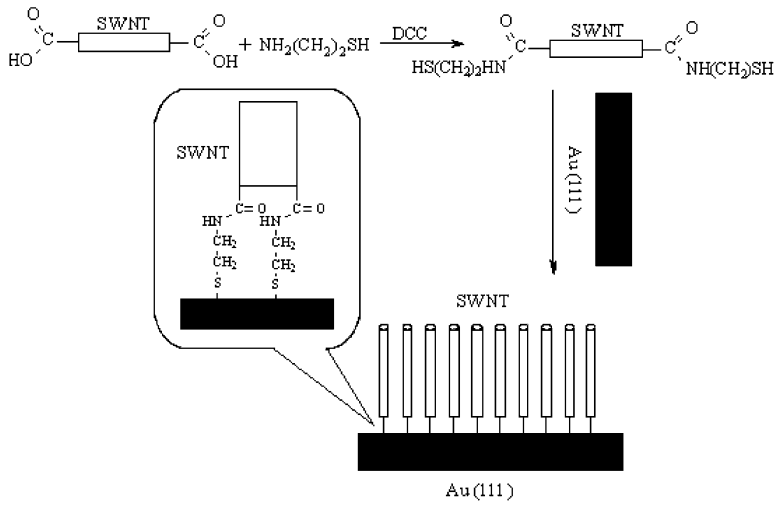

Figure 10. Synthesis of aligned SWNTs by the self-assembly of nanotubes end-functionalized with thiol groups on a gold substrate.

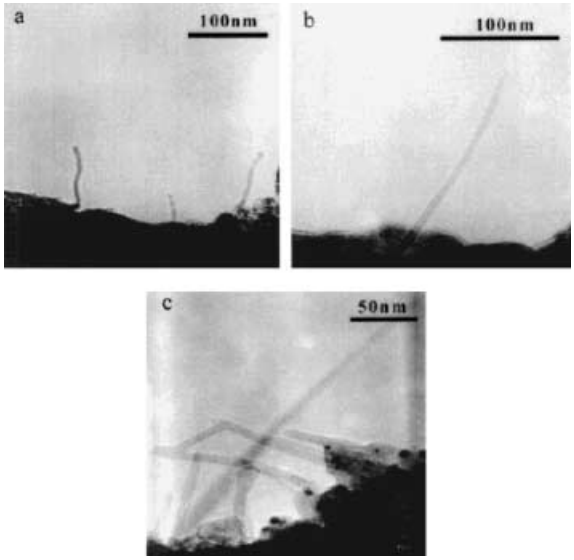

Figure 11. a) A shorter nanotube assembly with a lower packing density was formed with a shorter adsorption time whereas in b, c) a longer adsorption time resulted in the formation of an aligned nanotube array with a longer length and a higher packing density.[90]

The deprotonation between the carboxylic groups on the nanotubes and the metal surface effectively led to the anchoring, by Coulombic forces, of the aligned carbon nanotubes on the metal substrate via their carboxylated anion head groups. Raman spectroscopy seemed to support the process shown in Figure 12.[90]

More recently, Nan et al.[91] have demonstrated that *individual* acid oxidized SWNTs can be deposited onto a gold substrate that has been pretreated with $NH_2(CH_2)_{11}SH$ to form an aligned nanotube array on gold through the amide linkage. In this case, μCP was used to prepattern the thiol self-assembled monolayer on the gold surface for the region-specific deposition of the aligned carbon nanotubes. As shown in the optical microscope image (Figure 13a), the dark-dot regions are covered by carbon nanotubes. The corresponding AFM image given in Figure 13b clearly shows the aligned structure.

3.4. Micropatterns of Perpendicularly Aligned Carbon Nanotubes

On further investigation of the growth of aligned carbon nanotubes by the pyrolysis of FePc, we, among with others,[84–87] have also prepared micropatterns of *aligned* carbon nanotubes normal to the substrate surface suitable for field emission.[58] In particular, we have developed a novel method for the photolithographic generation of perpendicularly aligned carbon nanotube arrays with resolutions down to the micrometer scale.[92]

In the photolithographic approach, we first photolithographically patterned a positive photoresist film

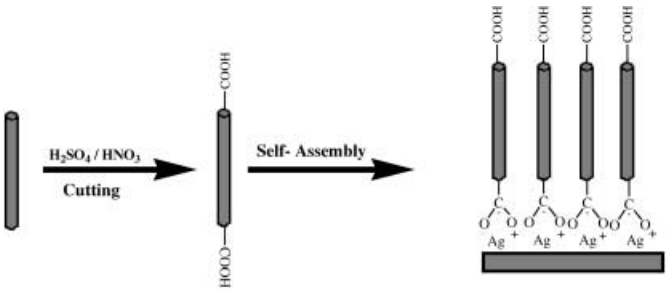

Figure 12. Diagram showing the anchoring of the aligned carbon nanotubes onto the metal substrate via their carboxylated anion head-groups.[91]

of diazonaphthoquinone (DNQ)-modified cresol novolak (Scheme 1a) onto a pristine quartz substrate. Upon UV irradiation through a photomask, the DNQ-novolak photoresist film in the exposed regions was rendered soluble in an aqueous solution of sodium hydroxide due to the photogeneration of the hydrophilic indenecarboxylic acid groups from the hydrophobic DNQ via a photochemical Wolff rearrangement (Scheme 1).[93] In this case, the photolithographically patterned photoresist film, after an appropriate carbonization process, acts as a shadow mask for the patterned growth of the aligned nanotubes. Figure 14a shows the steps of the photolithographic process. As can be seen, we carried out the pyrolysis of FePc onto the photoresist-prepatterned quartz plate after carbonization, leading to the region-specific growth of the aligned carbon nanotubes in the UV-exposed regions (Figure 14b). This method is fully compatible with existing photolithographic processes.[94]

Using a modified photolithographic method for the patterned pyrolysis of FePc, we have recently prepared *three-dimensional* micropatterns of *aligned* carbon nanotubes normal to the substrate surface with region-specific tubular lengths and packing densities. The photoresist system used in this approach

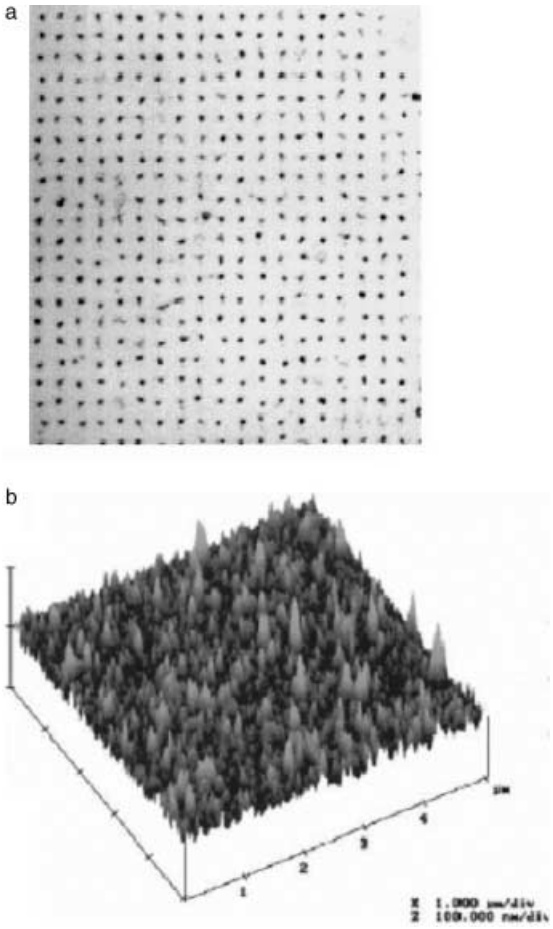

Figure 13. Perpendicularly aligned carbon nanotubes formed by the self-assembly of COOH-terminated nanotubes onto a gold surface prepatterned with thiol molecules. a) Optical microscope image and b) AFM image.[91]

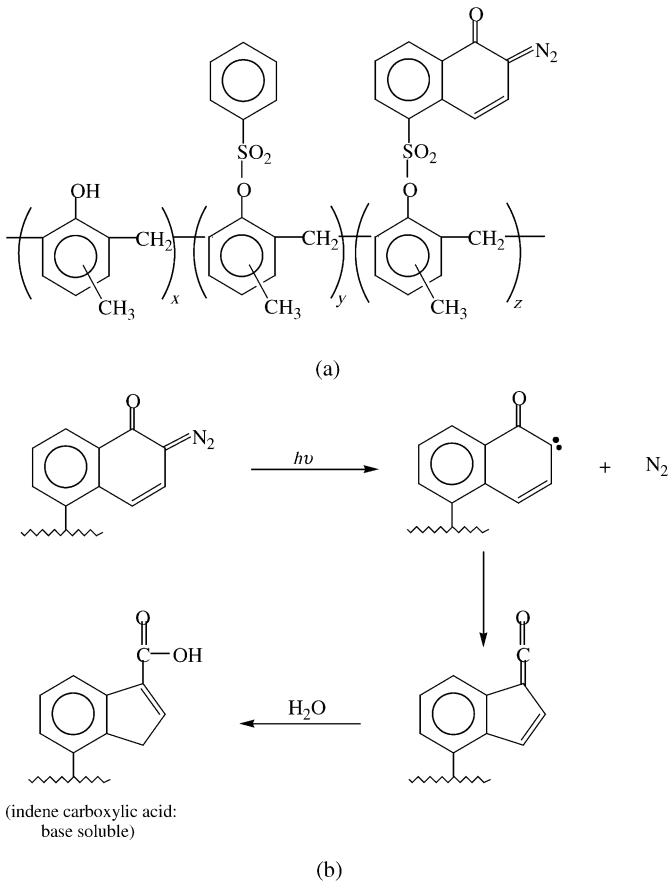

Scheme 1.

consists of novolac/hexamethoxymethyl melamine (HMMM) as the film former, phenothiazine (RH) as the photosensitizer, and diphenyliodonium hexafluorophosphate ($Ph_2I^+X^-$) as a photoacid generator that can photochemically generate the acid, through a photomask, required for the region-specific crosslinking of the photoresist film.[95] Figure 15 represents the steps of the photolithographic process with the associated photochemical reactions shown in Scheme 2.

UV irradiation through a photomask creates a latent acid pattern, formed by the photolithographic generation of acid from $Ph_2I^+X^-$ (Reaction (1) of Scheme 2). Postexposure baking at 110°C for 10 min (Figure 15) caused an acid-induced crosslinking of the novolac resin and HMMM (Reactions (2) and (3) of Scheme 2), rendering the photoresist film in the UV-exposed regions insoluble in an aqueous solution of sodium hydroxide (3 wt.-%) and ethanol (10 wt.-%). In contrast, the photoresist film in the regions not exposed to the UV light was removed simply by immersing in the developer solution for 10 – 20 s, which lead to the formation of a negative polymer pattern on the substrate. The crosslinking reactions between the HMMM and novolac resin were further completed by immersing the photoresist-patterned substrate in an aqueous solution of *p*-toluenesulfonic acid (10 wt.-%) for 30 min and baking at 150°C for 30 min.[95]

The photoresist-prepatterned silica wafer or quartz plate was then directly used as the substrate for the region-specific growing of aligned carbon nanotubes. Figure 16 represents a typical SEM image of the three-dimensional aligned carbon nanotube micropatterns thus prepared, which clearly shows a region-specific packing density and tubular length. In contrast to the DNQ-novolak photoresist film, the resultant HMMM-crosslinked novolac photoresist film supported the nanotube growth, most probably due to its delicate surface characteristics that allowed the Fe nanoparticles to deposit onto this particular photoresist layer at the initial stage of the FePc pyrolysis.[95] The 3D micropatterns of aligned carbon nanotubes thus prepared offer the possibility of constructing advanced microdevices with multidimensional features.

Recently, we have also used μCP and micromolding techniques to prepare micropatterns of carbon nanotubes aligned in a direction normal to the substrate surface.[96] Whereas the μCP process involves the region-specific transfer of self-assembling monolayers (SAMs) of alkylsiloxane onto a quartz substrate and the subsequent adsorption of polymer chains in the SAM-free regions (Figure 17a), the micromolding method allows the formation of polymer patterns through solvent evaporation from a precoated thin layer of polymer solution confined

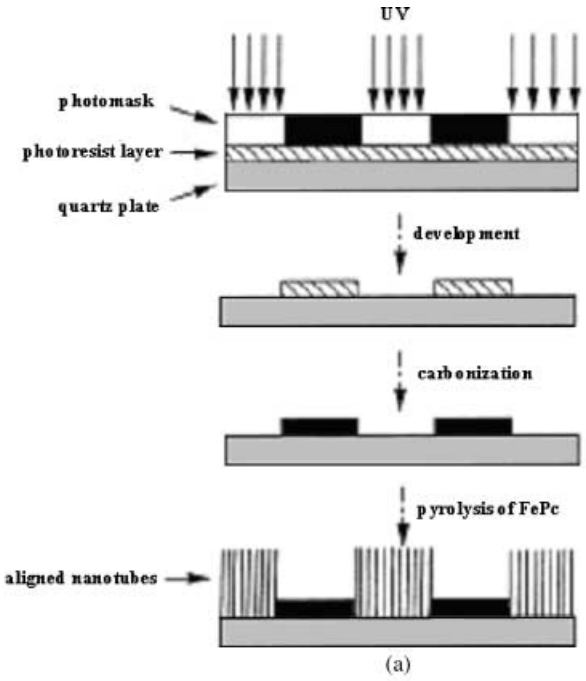

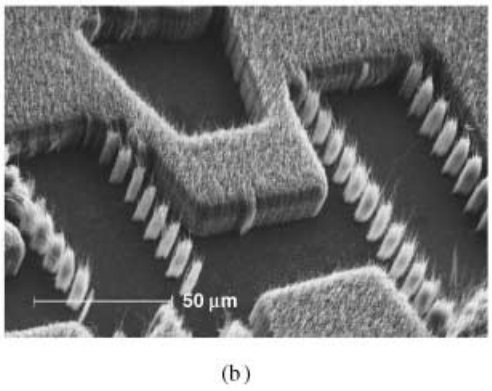

Figure 14. *a) Schematic representation of the micropattern formation of aligned carbon nanotubes by the photolithographic process. b) Typical SEM micrographs of patterned films of aligned nanotubes prepared by the pyrolysis of FePc onto a photolithographically prepatterned quartz substrate.*[92]

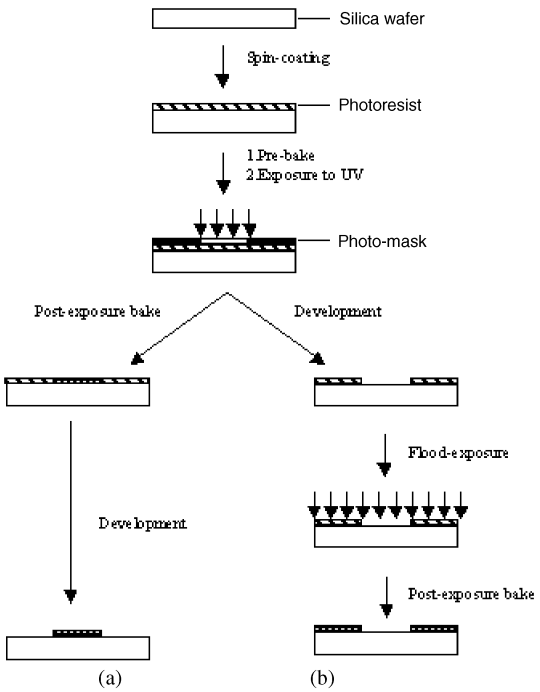

Figure 15. *Schematic illustration of the procedures for the photolithographic patterning of the chemically amplified photoresist into a) a negative and b) a positive pattern.*[95]

between a quartz plate and a polydimethylsiloxane (PDMS) elastomer mold (Figure 17b).

The DNQ-novolak photoresist patterns formed in both cases were then carbonized into carbon black for the region-specific growth of the aligned nanotubes in the polymer-free regions by pyrolysis of FePc under Ar/H_2 atmosphere at 800–1100°C, as is the case for the above mentioned photolithographic patterning. The spatial resolution was limited by the resolution of the mask used. As shown in Figure 18, micropatterns of aligned nanotubes thus prepared have resolutions down to 0.8 μm, suitable for the fabrication of various electronic and photonic devices. Kind et al.[97] have also used μCP to pattern catalysts for the region-specific growth of aligned carbon nanotubes. The ease with which micro-/nanopatterns of organic materials can be made even on curved surfaces by the soft lithographic techniques[98, 99] should provide additional benefits to this approach with respect to the photolithographic method, especially for the construction of flexible devices.

As can be seen from the above discussion, both the photolithographic and soft-lithographic patterning methods involve a tedious carbonization process prior to the aligned nanotube growth. In order to eliminate the carbonization process, we

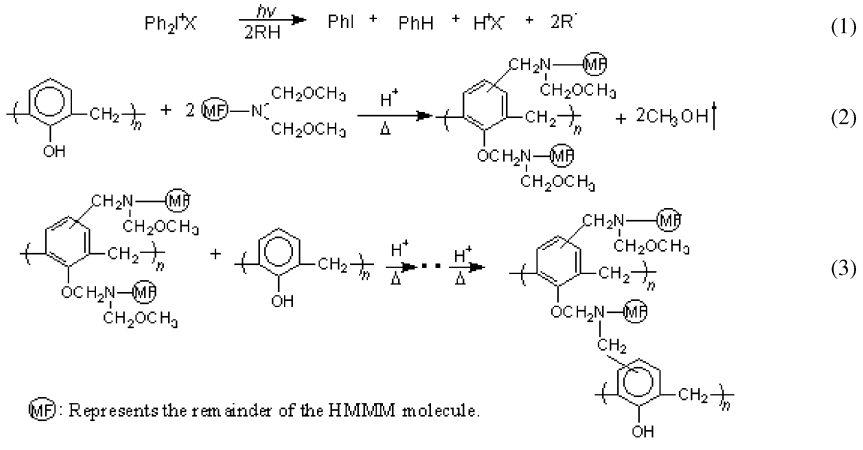

Scheme 2.

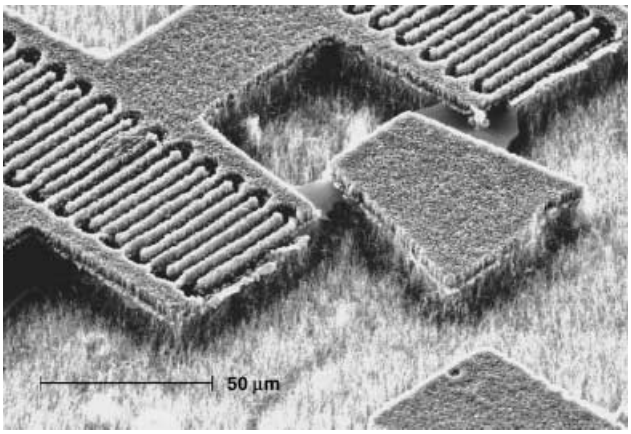

Figure 16. *A typical SEM image of the 3D-aligned carbon nanotube micropattern.*[95]

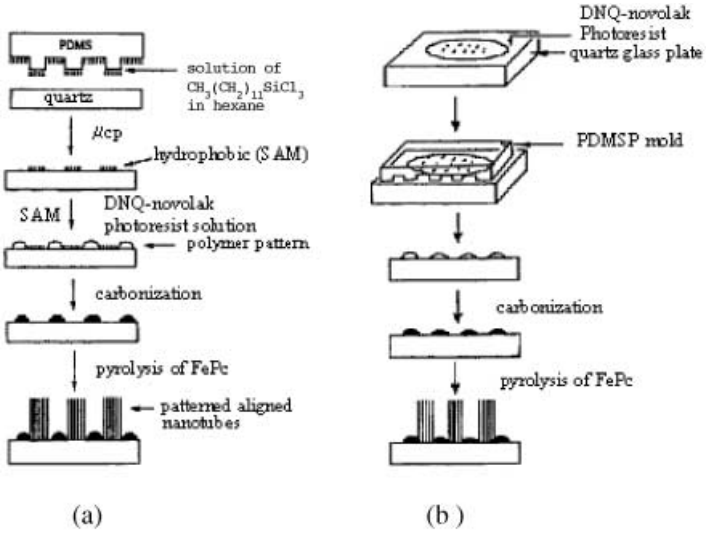

Figure 17. *Schematic illustration of the procedure for fabricating patterns of aligned carbon nanotubes by a) microcontact printing; b) solvent-assisted micromolding.*[96]

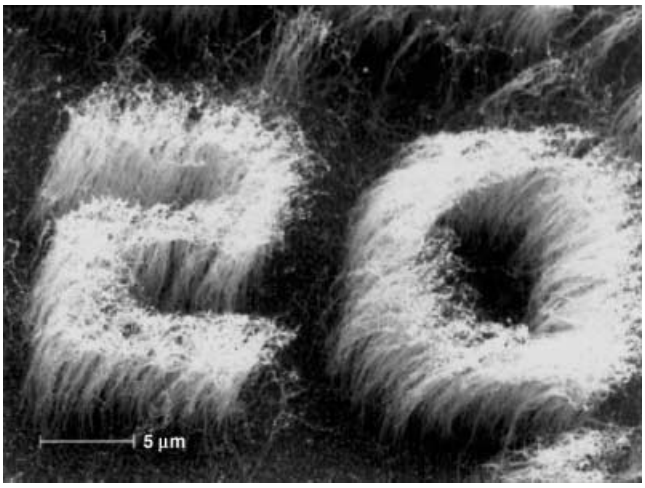

Figure 18. *A typical SEM image of an aligned nanotube pattern prepared by the pyrolysis of FePc onto the photoresist prepatterned quartz via micromolding.*[96]

prepared high-resolution carbon nanotube arrays aligned in a direction normal to the substrate surface by radiofrequency glow-discharge plasma polymerization of a thin polymer pattern onto a quartz substrate, followed by region-specific growth of the aligned carbon nanotubes in the plasma-polymer-free regions by the pyrolysis of FePc[58] (Figure 19).

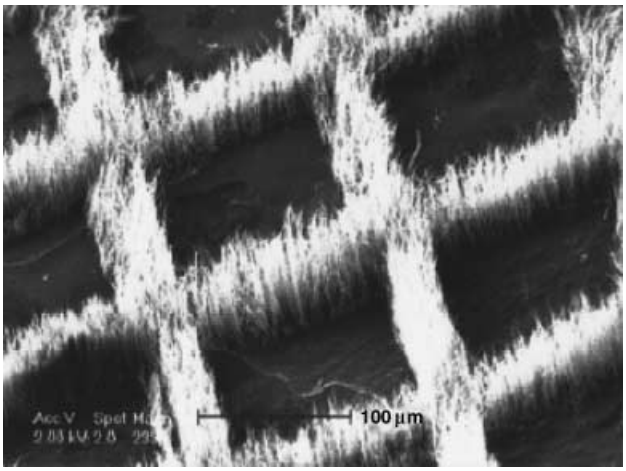

Figure 19. *SEM images of aligned carbon nanotube arrays growing out from the plasma-polymer-free regions.*[56]

The highly crosslinked structure of *n*-hexane-plasma-polymer films (prepared at 150 kHz, 60 W, and a monomer pressure of 15 torr for 5 min)[100, 101] could ensure the integrity of the plasma polymer layer, even without carbonization, at the high temperatures necessary for the nanotube growth from FePc. Therefore, the carbonization processes involved in our previous work on photolithographic[92] and soft-lithographic[96] patterning of the aligned carbon nanotubes can be completely eliminated in the plasma patterning process. Owing to the generic nature characteristic of the plasma polymerization, many other organic vapors could also be used efficiently to generate plasma polymer patterns for the patterned growth of aligned carbon nanotubes.

Many other groups have also devoted a great deal of effort to the micropatterning of carbon nanotubes. For example, Zhao and co-workers[102] used the micromolding in capillaries (MIMIC) technique, combined with 3D cubic mesoporous silica films containing catalysts, to fabricate microscopically ordered, aligned carbon nanotube patterns. In this case, a poly(dimethylsiloxane) (PDMS) mould having a patterned relief structure on its surface was placed on the surface of a substrate to form a network of channels between them. A solution mixture of a silica precursor, a PPO – PEG copolymer as the structure-directing agent, and ferric chloride was placed at the open ends of the channels; the liquid filled the channels by capillarity. After evaporating the solvent, the PDMS mould was carefully removed, which lead to a patterned film of mesoporous silica material on the surface of the substrate. The film was calcined to remove the copolymer and thereby produced patterned, mesoscopically ordered porous solids. The substrate was then placed in a furnace, followed by the reduction and deposition of carbon nanotubes. This provided a new, easy method for

controlling the orientation of aligned carbon nanotubes (by utilizing the catalysts incorporated into the ordered mesopores) with molecularly well-defined structures.[102] Fan et al.[84] reported the synthesis of massive arrays of monodispersed carbon nanotubes on a patterned porous silicon substrate with Fe films by electron beam evaporation through shadow masks. Sohn et al.[103, 104] have also used a similar method to produce aligned carbon nanotubes on Fe nanoparticles deposited by a pulsed laser on a porous Si substrate. They found that the growth characteristics of the carbon nanotubes depended strongly on the Fe film deposition (by the pulse-laser) time.[103, 104] Furthermore, Ren and co-workers[86, 105] reported the growth of free-standing multiwall carbon nanotubes onto a grid of patterned submicron nickel dot(s) by plasma-enhanced hot-filament CVD using acetylene gas as the carbon source and ammonia as the dilution gas. Single carbon nanotubes were observed to grow on the grid and they separated well (Figure 20). A thin film nickel grid was fabricated on a silicon wafer by electron beam lithography and metal evaporation. Using this method, free-standing vertical carbon nanotubes (Figure 20) suitable for certain specific applications, such as scanning microscopy probes and electron emitters, were fabricated.[86, 105]

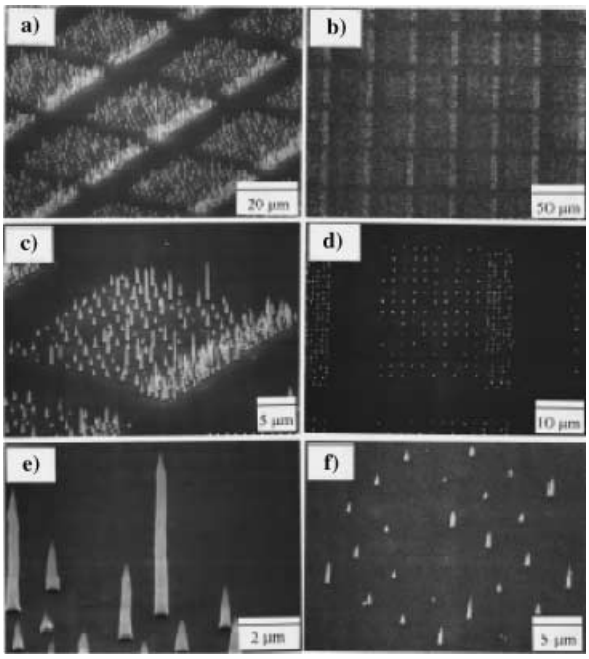

Figure 20. *A series of SEM images from different viewing angles showing the growth of carbon nanotube obelisks on an array of submicron nickel dots. a) An inclined view of a repeated array pattern. b) A top (normal) view of a repeated array pattern. c) An inclined view of one array pattern. d) A top (normal) view of one array pattern. e) A magnified view along the edge of one pattern. f) An inclined view of carbon obelisks grown on nickel dots separated by 5 μm.*[86]

Teo et al.[106] also fabricated a uniform array of nanotubes of single, free-standing aligned carbon nanotubes by plasma-enhanced CVD with either photolithographically (or electron-beam lithographically) patterned nickel catalyst substrates (Figure 21).[106]

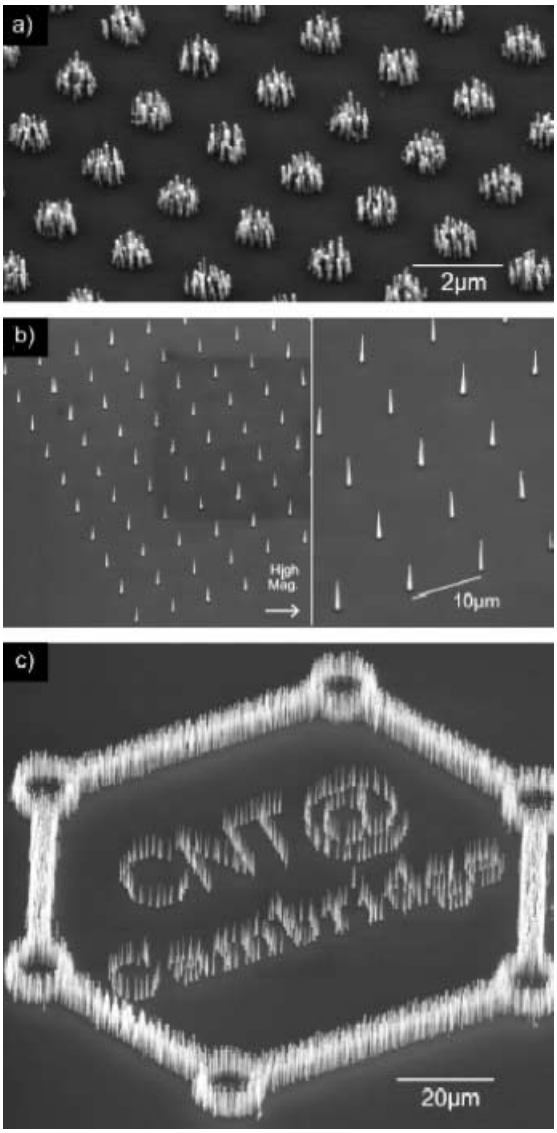

Figure 21. *a) Bunches of aligned carbon nanotubes (about 100 nm) are deposited on 1 μm nickel dots by breaking up the nickel catalyst film into multiple nanoparticles. b) Single aligned nanotubes are deposited when the nickel dot size is reduced to 100 nm as only a single nickel nanoparticle is formed from the dot. c) The selective growth of high yield and uniform aligned nanotubes with different densities.*[106]

Although a micropore template, such as mesoporous silicon or aluminum oxide film, provided a simple way to synthesize aligned carbon nanotubes, the characteristics of the template played a key role in the production of the aligned carbon nanotubes. Recently, Ajayan and co-workers[107] have reported the highly substrate-dependent site-selective growth of aligned carbon nanotubes by CVD on patterned SiO_2/Si substrates using conventional lithography. SEM results indicated that carbon nanotubes grew on the SiO_2 substrate, with no observable growth on the Si substrate. More recently, these authors have used photolithography to pattern a silicon surface with silica (SiO_2) polygons to allow the aligned carbon nanotubes to grow out in several different directions at once (Figure 22).[108, 109]

Figure 22. Multidimensional aligned carbon nanotubes grown out from SiO_2 polygons prepatterned on a Si substrate.[108]

3.5. Modification of Perpendicularly Aligned Carbon Nanotubes

3.5.1. Plasma Etching To Open the Aligned Carbon Nanotube Tips

We have previously reported that H_2O-plasma can be used to effectively etch many substrates including mica sheets.[100] We found that H_2O-plasma etching can also be used to selectively open the top end-caps of the perpendicularly aligned carbon nanotubes without any observable structural change for the sidewalls, under appropriate plasma conditions. Figure 23a shows the typical closed structure of the as-grown aligned carbon nanotubes with encapsulated Fe rods at their tips. In contrast, Figure 23b clearly shows the removal of the top end-caps from the aligned nanotubes by the H_2O-plasma.

3.5.2. Plasma Activation of Aligned Carbon Nanotubes for Chemical Modification

The plasma technique has also been known to play an important role in the surface activation of various materials, ranging from organic polymers to inorganic ceramics and metals.[100, 101] As can be seen from the above discussion, H_2O-plasma etching can be used to open the aligned carbon nanotubes, and hence allow the chemical modification of the inner, outer, or both surfaces of the nanotubes. In view of the fact that acetaldehyde plasma has been used for the surface modification of biomaterials,[111] we have developed a novel approach for chemically modifying carbon nanotubes by activating them with an acetaldehyde plasma followed by chemical reactions characteristic of the plasma-generated functional groups.[112] For instance, amino-dextran chains have been successfully immobilized onto acetaldehyde-plasma-treated aligned carbon nanotubes through the formation of a Schiff-base linkage, which was further stabilized by reduction with sodium cyanoborohydride (Scheme 3).[112, 113] The polysaccharide-grafted nanotubes are very hydrophilic: potentially useful for many biological applications.

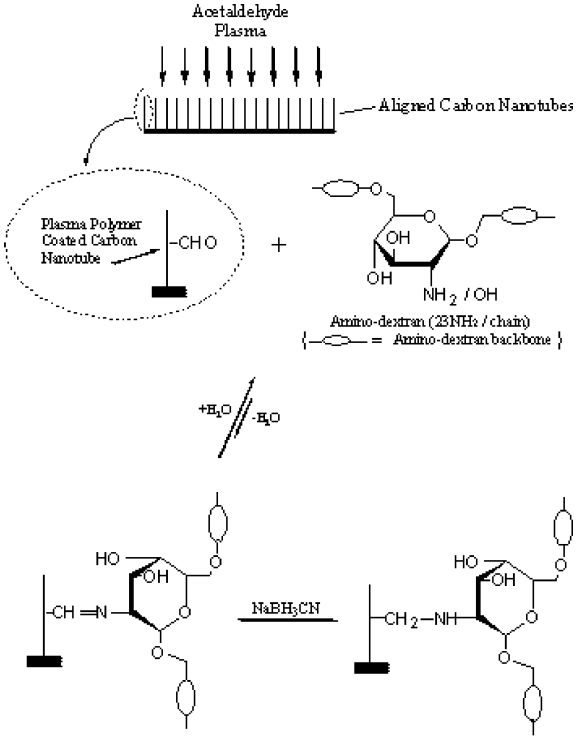

Scheme 3.

3.5.3. Electrochemical Coating of the Aligned Carbon Nanotubes with Conducting Polymers

Recently, we have also used the aligned carbon nanotubes produced from FePc to make novel conducting polymer–carbon nanotube (CP–NT) coaxial nanowires by electrochemically depositing a concentric layer of an appropriate conducting polymer uniformly onto each of the constituent aligned nanotubes.[114]

The SEM image for the CP–NT coaxial nanowires given in Figure 24b shows the same features as the pristine aligned nanotube array of Figure 24a, but with a larger diameter due to

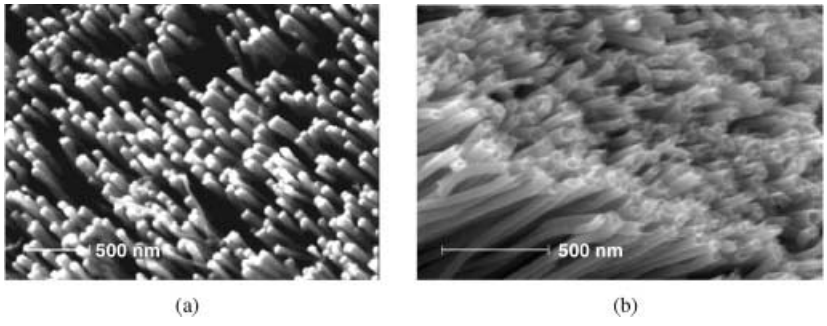

Figure 23. Aligned carbon nanotubes a) before and b) after tip removal by water plasma etching.[110]

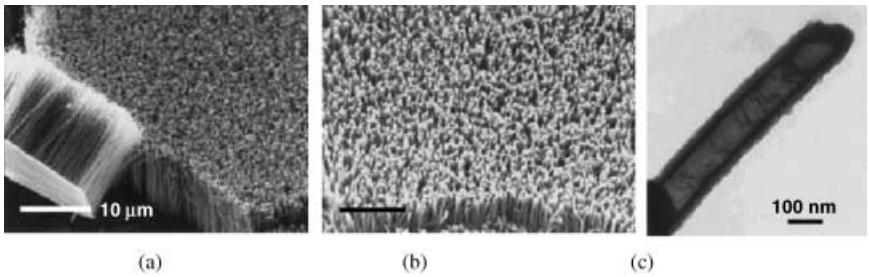

Figure 24. Aligned carbon nanotubes a) before and b) after electrochemical coating with a concentric polypyrrole layer. c) A typical TEM image of the CP – NT coaxial nanowire at the tip region.[114]

the presence of the newly electropolymerized polypyrrole coating in this particular case. The formation of the conducting polymer layer was also evidenced by TEM images (Figure 24c).[114]

The electrochemical performance of the aligned CP – NT coaxial nanowires was evaluated by carrying out cyclic voltammetry measurements. As for polyaniline films electrochemically deposited on conventional electrodes, the cyclic voltammetric response of the polyaniline coated nanotube array in an aqueous solution of 1 M H_2SO_4 (Figure 25a) shows oxidation peaks at 0.33 and 0.52 V (but with much higher current densities).[114] As a

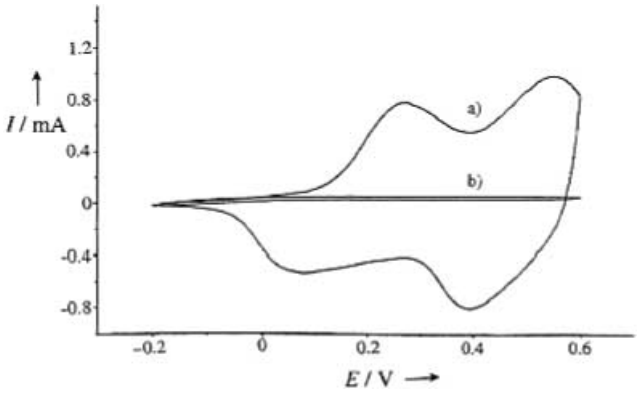

Figure 25. Cyclic voltammograms of a) the polyaniline-coated CP – NT coaxial nanowires and b) the bare, aligned carbon nanotubes. Measured in an aqueous solution of 1 M H_2SO_4 with a scan rate of 50 mV s^{-1}.[114]

control, the cyclic voltammetry measurement was also carried out on the bare aligned nanotubes under the same conditions (Figure 25b). In the control experiment, only capacitive current was observed, with no peak attributable to the presence of any redox active species. The coaxial structure allows the nanotube framework to provide mechanical stability[115, 116] and efficient thermal/electrical conduction[115, 117] to and from the conducting polymer layer.

The large surface/interface area obtained for the nanotube-supported conducting polymer layer is an additional advantage for using them in many optoelectronic applications, for example, in organic light-emitting diodes and photovoltaic cells where the charge injection and separation are strongly limited by the interfacial area available in more conventional devices.[118, 119]

3.5.4 Acid Oxidation with Structural Protection

In view of the fact that a simple application of the solution-acid-oxidization of nanotubes[57] to aligned carbon nanotubes for generating carboxy and/or hydroxy groups for further chemical modification often leads to total collapse of the aligned nanotubes, Meyyappan and co-workers[120] developed an effective method for protecting the alignment structure by filling the gaps between the aligned nanotubes with a spin-on glass (SOG) prior to the oxidative reaction (Figure 26).

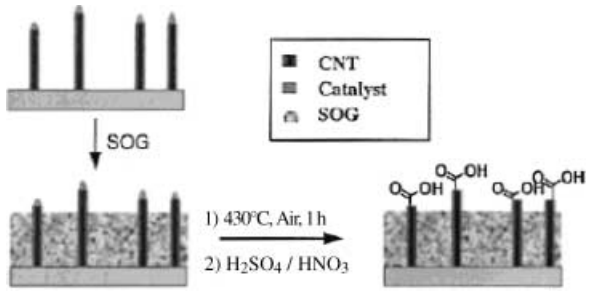

Figure 26. Schematic representation of the fabrication and pretreatment of the aligned carbon nanotubes for further functionalization.[120]

Figure 27 shows the oxidation-induced changes in alignment for the aligned carbon nanotubes with and without the SOG protection. Compared to Figure 27b, Figure 27c indicates that the SOG film provides structural support to the aligned carbon nanotubes.

After having successfully functionalized the tips of the aligned carbon nanotubes with carboxy groups, these authors further demonstrated accomplishments in chemical coupling of nucleic acids to the aligned nanotube array using the standard water soluble coupling reagents [that is, 1-ethyl-3-(3-dimethylaminopropyl) carbodiimide hydrochloride, EDC, and *N*-hydroxysulfosuccinimide, sulfo-NHS], as schematically shown in Scheme 4.

4. Aligned Noncarbon Nanotubes

Just as carbon nanotubes have attracted a great deal of research activity, the investigation of noncarbon nanotubes has also generated a large number of publications.[10, 11, 121–124] Below, we will highlight some important work on noncarbon nanotubes with a few examples.

4.1. Aligned Inorganic Nanotubes

Gong et al.[125] fabricated well-aligned titanium oxide nanotubes by the anodic oxidation of a pure titanium sheet in an aqueous

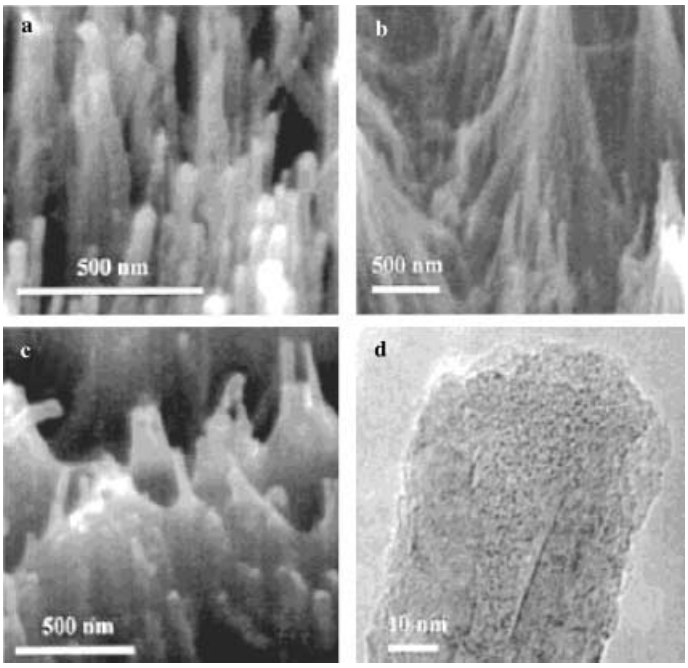

Figure 27. *SEM images of a) Vertically aligned carbon nanotube arrays. b) The collapsed carbon nanotube array without SOG after the oxidative treatment. c) The aligned carbon nanotube array with SOG after the oxidative treatment. d) High-resolution TEM image of the opened carbon nanotube.*[120]

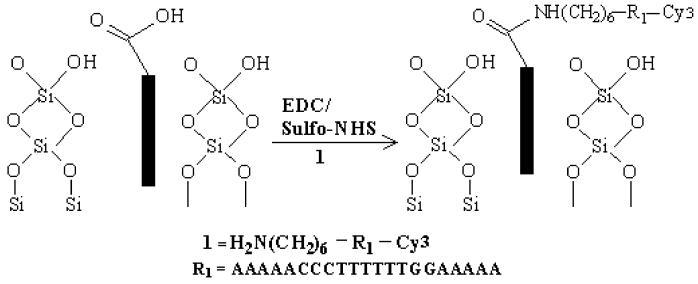

Scheme 4.

solution containing 0.5 to 3.5 wt.-% hydrofluoric acid. The aligned nanotubes can organize into high-density uniform arrays with opened top-tips and closed bottom-tips. The average tube diameter was in the range of 25 – 65 nm, and it was found to increase with the increasing anodizing voltage.

Bao et al.[126] prepared highly ordered magnetic Ni nanotubules up to 35 μm in length and 160 nm in outer diameter by electrodeposition in the pores of an alumina membrane modified with an organoamine as a pore-wall modifying agent. The coercivity of the nanotubules was enhanced compared with that of the bulk nickel. These authors believed that such metal nanotubules could have a variety of promising applications, including use as porous electrodes, multilayer nanostructures for information storage by filling with ferromagnetic and non-magnetic metals, and novel nanocomposite materials by filling with other materials of specific magnetic, optical, and/or electrical properties. They have also obtained arrays of polyaniline nanotubules within the pores of an alumina template membrane and filled iron, nickel, and cobalt nanowires into the nanotubules of polyaniline.

Michailowski et al.[127] prepared compact, continuous, and uniform anatase nanotubules by impregnating the porous anodic alumina pores with titanium isopropoxide and then oxidatively decomposing the reagent at 500°C. The uniform anatase nanotubes thus obtained have diameters in the range of 50 – 70 nm. Repeated filling of the template pores was demonstrated to be feasible with an increment in the wall thickness of $\sim$3 nm per impregnation. These authors have also used CVD to create alternating metallic (carbon) and insulating (boron nitride) layers within the template pores in anodic aluminum oxide templates.[128] The resultant composite metal/insulator/metal nanotubules can be converted to an array of nanocapacitors connected in parallel, attaining specific capacitances of up to 2.5 μF cm^{-2} for a 50 μm thick template.

Rao and co-workers[129a] have recently obtained aligned boron nitride nanotubes by simply heating the aligned multiwalled carbon nanotubes and boric acid together over 1000 – 1300°C. The aligned boron nitride nanotubes have an average outer diameter of $\approx$15 – 40 nm. Aligned multiwall carbon nanotubes have also been used as reacting templates for the formation of aligned multiwall BN nanotubes in the presence of boron oxide and metal oxide promoters.[129b]

4.2. Aligned Polymer Nanotubes

Carbon nanotubes, consisting of hexagons arranged in a concentric manner with a conjugated all-carbon structure, can be regarded as the newest members of the polymer family. On the other hand polymers offer a unique class of material with the natural length of polymer chains, and their morphologies in the bulk, lying precisely at the nanometer length scale, indicating a considerable room for creating new nanostructures of useful properties and functions even without any change in their chemical composition. Indeed, the systematic organization of biopolymers on the nanometer length scale is a key feature of biological systems.

4.2.1. Template Synthesis of Aligned Polymer Nanotubes

Polymer nanowires with nanometer-scale architectures have been fabricated by using porous membranes or supramolecular nanostructures as templates. For instance, Smith et al.[130] have recently developed a process for producing nanocomposites with well-defined poly(*p*-phenylene vinylene), PPV, nanowires within self-organizing liquid-crystal matrixes. This process involves the self-assembly of a polymerizable liquid-crystal monomer (for example, acrylate) into an ordered hexagonal array of hydrophilic channels (about 4 nm in diameter) filled with a precursor polymer of PPV, followed by photopolymerization to lock-in the matrix architecture and then thermal conversion to form PPV nanofibers in the channels. As a result, significant fluorescence enhancement was observed, most probably due to

the much reduced interchain-exciton quenching achieved by separating the PPV molecules from the polymer matrix. Shi and co-workers[131] prepared aligned polythiophene micro- and nanotubules through the electrochemical oxidation of thiophene directly within nanoscale microporous alumina membranes precoated with gold. By so doing, these authors obtained films of polythiophene/gold bilayer micro- or nanotubules with a strong redox response and a large charge/discharge capacity: about 30 times higher than that of polythiophene films prepared by conventional electrochemical polymerization.

More generally, polymer nanowires and nanotubes with improved order and fewer structural defects can be synthesized within a template formed by the pores of a nanoporous membrane[132] or the nanochannels of a mesoporous zeolite.[133] Template synthesis often allows for the production of polymeric wires or tubules with controllable diameters and lengths (Figure 28).[134] Template synthesis of conjugated polymers,

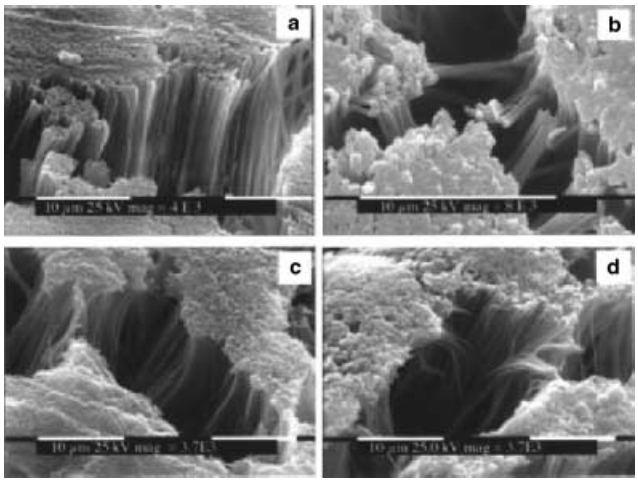

Figure 28. *SEM images of microfibrils prepared in an alumina template membrane: a) polystyrene, PS; b) poly(vinylidene fluoride), PVDF; c) poly(phenylene oxide); and d) poly(methyl methacrylate), PMMA.*[134]

including polyacetylene, polypyrrole, polythiophene, polyaniline, and PPV may be achieved by electrochemical or chemical oxidative polymerization of the corresponding monomers. Whereas an electrochemical template synthesis can be carried out within the pores of a membrane that has been precoated with a metal on one side (as the anode),[132] a chemical template synthesis is normally performed by immersing the membrane into a solution containing the desired monomer and an oxidizing agent, with each of the pores acting as a tiny reaction vessel.

It has been noted with interest that if the pores of polycarbonate membranes are used as the template, highly ordered polymeric tubules are produced by preferential polymerization along the pore walls due to the specific solvophobic and/or electrostatic interactions between the polymer and the pore wall.[135] These conducting polymer tubules show a wide range of electrical conductivities, which increase with decreasing pore diameter.[136] This is because the alignment of the polymer chains on the pore wall can enhance conductivity, and the smaller tubules contain proportionately more of the ordered material.

By wetting ordered porous templates with polymer solution or melts, Steinhart et al.[137] developed another simple technique for the fabrication of polymer nanotubes with a monodisperse size distribution and uniform orientation. Figure 29 shows polymer nanotubes formed by the melt-wetting of ordered

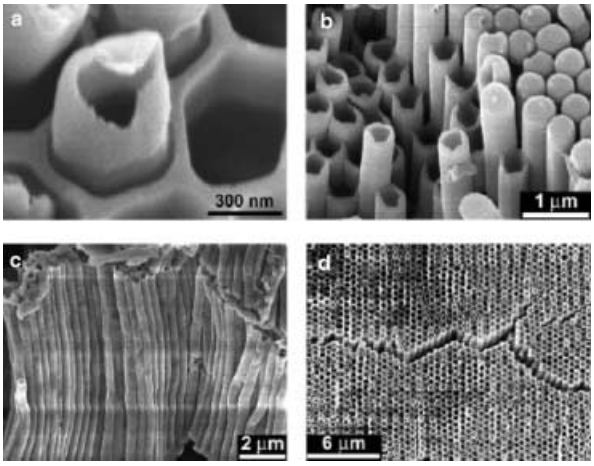

Figure 29. *SEM images of nanotubes obtained by melt-wetting. A) Damaged tip of a PS nanotube. B) Ordered array of tubes from the same PS sample after complete removal of the template. C) Array of aligned polytetrafluoroethylene, PTFE, tubes. D) PMMA tubes (with long-range hexagonal order) obtained by wetting a macroporous silicon pore array and after complete removal of the template.*[137]

porous alumina and oxidized macroporous silicon templates with a narrow pore size distribution. This method can be used to produce polymer nanotubes of a narrow size distribution from almost all melt-processible polymers, their blends, or multicomponent solutions.

These studies are of particular interest because high-temperature graphitization of the polymer nanotubes could transform them into carbon nanotubes of superior electronic and mechanical properties, as demonstrated by the polyacrylonitrile (PAN) nanotubules synthesized in the pores of an alumina membrane or in zeolite nanochannels.[138, 139]

4.2.2. Template-Free Synthesis of Aligned Polymer Nanotubes

More recently, conjugated conducting polymer nanotubes were synthesized using "template-free" polymerization that involves a self-assembled supramolecular template.[140, 141] Without using any templates, for example, Wan and co-workers[140] synthesized polyaniline (PANI) *nanotubes* (Figure 30) via a solution chemistry using $(NH_4)_2S_2O_8$ as the oxidant in the presence of a self-assembled $C_{60}(OH)_6(OSO_3H)$. More recently, Shi and co-workers[142] have developed an eletrochemical technique to grow perpendicularly aligned conducting polymer nano-/microstructures.

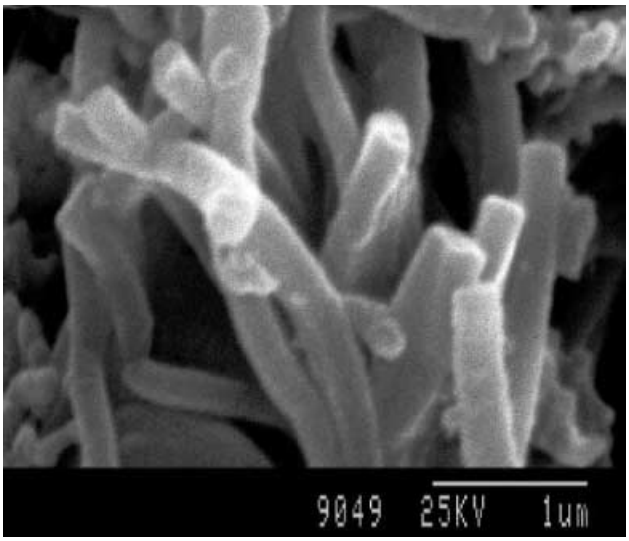

Figure 30. *SEM image of PANI-$C_{60}(OH)_6(OSO_3H)_6$ nanotubes.*[140]

4.2.3. Aligned Peptide Nanotubes

Nanotubes constructed with peptides offer a new, very powerful approach to treating bacterial infections.[143, 144] These nanotubes are formed by the self-assembly of cyclic peptides with an even number of alternating D- and L-amino acids. The cyclic peptides are stable in solution when they are in an open, flat conformation with all the side chains pointing outwards. They stack by intermolecular hydrogen bonding through the amide backbone, forming a tube that resembles protein-sheets (Figure 31). The nanotubes are membrane active. They readily insert themselves into cell membranes and align perpendicularly to the membranes. Cells die instantly if their membranes become permeable and leaky. Ghadiri's cyclic peptides assemble to a higher-order structure, like the nanotubes, and it is that structure which kills the bacteria, not the single molecule. This is an entirely new concept in pharmaceutical research and development. The researchers have successfully designed the right peptides that form nanotubes in bacterial cell membranes only and exclusively to kill bacterial cells. Continued research effort in this embryonic field could give birth to a flourishing area of biotechnology.

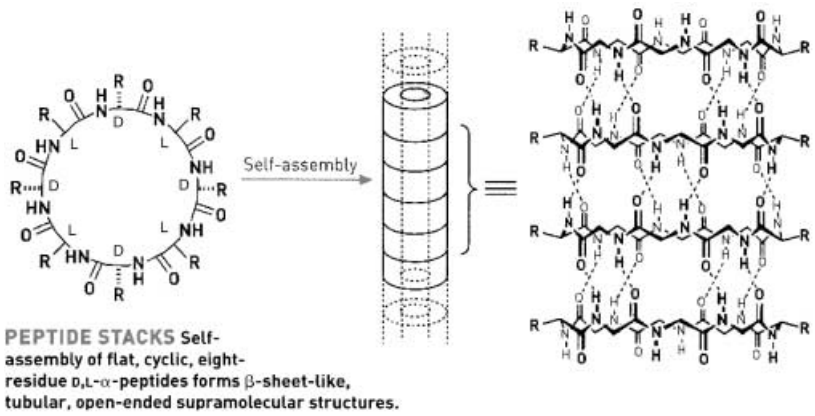

Figure 31. *A schematic representation of aligned peptide nanotubes formed by self-assembly.*[144]

5. Conclusion

As can be seen from the above discussion, their peculiar hollow geometry, coupled with a layered cylindrical structure, has made carbon nanotubes and their noncarbon counterparts exhibit many new intriguing electrical, mechanical, and thermal properties with respect to those more conventional counterparts. Various synthetic and microfabrication techniques have been developed for preparing aligned and micropatterned nanotubes with desirable structural/property characteristics. The aligned and micropatterned structure also facilitated the controlled structural modifications of nanotubes for specific applications. Recent development in the field has clearly indicated the possibility of developing a wide range of nanotube architectures with desirable features by their controlled synthesis and microfabrication. With the promising approaches already reviewed in this article, and more to be developed, practical applications of the aligned and/or micropatterned nanotubes are imminent.

Keywords: alignment · nanotubes · patterning · photolithography · self-assembly · soft-lithography

[1] *Nanotechnology* (Ed.: G. L. Timp), Springer-Verlag, New York, **1998**.
[2] A. N. Goldstein, *Handbook of Nanophase Materials*, Marcel Dekker, Inc., New York, **1997**.
[3] S. Iijima, *Nature* **1991**, *354*, 56.
[4] M. S. Dresselhaus, G. Dresselhaus, P. Eklund, *Science of Fullerenes and Carbon Nanotubes*, Academic Press, New York, **1996**.
[5] a) T. Ebbesen, *Carbon Nanotubes*, CRC Press, Boca Raton, FL, **1997**; b) C. N. R. Rao, B. C. Satishkumar, A. Govindaraj, M. Nath, *ChemPhysChem* **2001**, *2*, 79.
[6] R. Saito, G. Dreesselhaus, M. S. Dresselhaus, *Physical Properties of Carbon Nanotubes*, Imperial College Press, London, **1998**.
[7] W. A. de Heer, J. M. Bonard, K. Fauth, A. Châtelain, L. Forró, D. Ugarte, *Adv. Mater.* **1997**, *1*, 87.
[8] T. W. Ebbesen, *Phys. Today* **1996**, 26.
[9] P. R. Birkett, M. Terrones, *Chem. Brit.* **1999**, *May*, 45.
[10] V. V. Pokropivnyi, *Powder Metall. Met. Ceram.* **2001**, *40*, 9, and references therein.
[11] V. V. Pokropivnyi, G. S. Skorokhod, G. S. Oleinik, A. V. Kurdyumov, T. S. Bartniskaya, A. V. Pokropivny, A. G. Sisonyuk, D. M. Sheichenko, *J. Solid State Chem.* **2000**, *154*, 214.
[12] X. Blasé, J.-Ch. Charlier, A. De. Vita, R. Car, *Appl. Phys. A* **1999**, *68*, 293.
[13] S. J. Tans, A. R. M. Verschueren, C. Dekker, *Nature* **1998**, *393*, 49.
[14] A. N. Cleland, M. L. Roukes, *Nature* **1998**, *392*, 160.
[15] S. Frank, P. Poncharal, Z. L. Wang, W. A. de Heer, *Science* **1998**, *280*, 1744.
[16] H. Dai, J. H. Hafner, A. G. Rinzler, D. T. Colbert, R. E. Smalley, *Nature* **1996**, *384*, 147.
[17] R. Stevens, C. Nguyen, A. Cassell, L. Delzeit, M. Meyyappan, J. Han, *Appl. Phys. Lett.* **2000**, *77*, 3453.
[18] S. S. Wong, J. D. Harper, P. T. Lansbury Jr, C. M. Lieber, *J. Am. Chem. Soc.* **1998**, *120*, 603.
[19] S. S. Wong, E. Joselevich, A. T. Woolley, C. L. Cheung, C. M. Lieber, *Nature* **1998**, *394*, 52.
[20] T. Rueckers, K. Kim, E. Joselevich, G. Y. Tseng, C. L. Cheung, C. M. Lieber, *Science* **2000**, *289*, 94.
[21] W. A. de Heer, J. M. Bonard, K. Fauth, A. Châtelain, L. Forró, D. Ugarte, *Adv. Mater.* **1997**, *9*, 87, and references therein.
[22] H. Schmid, H. W. Fink, *Appl. Phys. Lett.* **1997**, *70*, 2679.
[23] Y. Saito, K. Hamaguchi, T. Nishino, K. Hata, K. Tohji, A. Kasuya, Y. Nishina, *Jpn. J. Appl. Phys.* **1997**, *36*, L1340.

[24] Q. H. Wang, T. D. Corrigan, J. Y. Dai, R. P. H. Chang, A. R. Krauss, *Appl. Phys. Lett.* **1997**, *70*, 3308.
[25] N. I. Sinitsyn, Y. V. Gulyaev, G. V. Torgashov, L. A. Chernozatonskii, Z. Y. Kosakovskaya, Y. F. Zakharchenko, N. A. Kiselev, A. L. Musatov, A. I. Zhbanov, S. T. Mevlyut, O. E. Glukhova, *Appl. Surf. Sci.* **1997**, *111*, 145.
[26] J. M. Bonard, F. Maier, T. Stöckli, A. Châtelain, W. A. de Heer, J. P. Salvetat, L. Forró, *Ultramicroscopy* **1998**, *73*, 7.
[27] G. E. Gadd, M. Blackford, S. Moricca, N. Webb, P. J. Evans, A. M. Smith, G. Jacobsen, S. Leung, A. Day, Q. Hua, *Science* **1997**, *277*, 933.
[28] A. C. Dillon, K. M. Jones, T. A. Bekkedahl, C. H. Kiang, D. S. Bethune, M. J. Heben, *Nature* **1997**, *386*, 377.
[29] C. Niu, E. K. Sichel, R. Hoch, D. Moy, H. Tennent, *Appl. Phys. Lett.* **1997**, *70*, 1480.
[30] G. Che, B. B. Lakshmi, E. R. Fisher, C. R. Martin, *Nature* **1998**, *393*, 346.
[31] A. Chambers, C. Park, R. Terry, K. Baker, N. M. Rodriguez, *J. Phys. Chem. B* **1998**, *102*, 4253.
[32] P. Chen, X. Wu, J. Lin, K. L. Tan, *Science* **1999**, *285*, 91.
[33] Z. F. Ren, *Technol. Rev.* **2000**, *January/February*, 25.
[34] R. H. Baughman, C. Cui, A. A. Zakhidov, Z. Iqbal, J. N. Barisci, G. M. Spinks, G. G. Wallace, A. Mazzoldi, D. De Rossi, A. G. Rinzler, O. Jaschinski, S. Roth, M. Kertesz, *Science* **1999**, *284*, 1340.
[35] L. Dai, P. Soundarrajan, T. Kim, *Pure Appl. Chem.* **2002**, *74*, 1753 – 1772, and references therein.
[36] J. M. Bonard, J. P. Salvetat, T. Stöckli, W. A. de Heer, L. Forró, A. Chatelain, *Appl. Phys. Lett.* **1998**, *73*, 918.
[37] Y. Satio, K. Hamaguchi, S. Uemura, K. Uchida, Y. Tasaka, F. Ikazaki, M. Yumura, A. Kasuya, Y. Nishina, *Appl. Phys. A* **1998**, *67*, 95.
[38] Y. Saito, S. Uemura, K. Hamaguchi, *Jpn. J. Appl. Phys.* **1998**, *37*, L346.
[39] Q. H. Wang, A. A. Setlur, J. M. Lauerhaas, J. Y. Dai, E. W. Seelig, R. P. H. Chang, *Appl. Phys. Lett.* **1998**, *72*, 2912.
[40] Y. Saito, S. Uemura, *Carbon* **2000**, *38*, 169.
[41] D. S. Chung, W. B. Choi, J. H. Kang, H. Y. Kim, I. T. Han, Y. S. Park, Y. H. Lee, N. S. Lee, J. E. Jung, J. M. Kim, *J. Vac. Sci. Technol. B* **2000**, *18*, 1054.
[42] W. B. Choi, D. S. Chung, J. H. Kang, H. Y. Kim, Y. W. Jin, I. T. Han, Y. H. Lee, J. E. Jung, N. S. Lee, G. S. Park, J. M. Kim, *Appl. Phys. Lett.* **1999**, *75*, 3129.
[43] D. Normile, *Science* **1999**, *286*, 2056.
[44] W. B. Choi, Y. H. Lee, N. S. Lee, J. H. Kang, S. H. Park, H. Y. Kim, D. S. Chung, S. M. Lee, S. Y. Chung, J. M. Kim, *Jpn. J. Appl. Phys. Part 1* **2000**, *39*, 2560.
[45] J. M. Kim, W. B. Choi, N. S. Lee, J. E. Jung, *Diamond Relat. Mater.* **2000**, *9*, 1184.
[46] J. L. Kwo, M. Yokoyama, W. C. Wang, F. Y. Chuang, I. N. Lin, *Diamond Relat. Mater.* **2000**, *9*, 1270.
[47] P. J. F. Harris, *Carbon Nanotubes and Related Structures—New Materials for the Twenty-First Century*, Cambridge University Press, Cambridge, **2001**.
[48] G. Che, B. B. Lakshmi, E. R. Fisher, C. R. Martin, *Nature* **1998**, *393*, 346.
[49] K. B. Jirage, J. C. Hulteen, C. R. Martin, *Science* **1997**, *278*, 655.
[50] W. A. de Heer, W. S. Bacsa, A. Châtelain, T. Gerfin, R. Humphrey-Baker, L. Forró, D. Ugarte, *Science* **1995**, *268*, 845.
[51] P. M. Ajayan, *Adv. Mater.* **1995**, *7*, 489.
[52] M. Terrones, N. Grobert, J. Olivares, J. P. Zhang, H. Terrones, K. Kordatos, W. K. Hsu, J. P. Hare, P. D. Townsend, K. Prassides, A. K. Cheetham, H. W. Kroto, D. R. M. Walton, *Nature* **1997**, *388*, 52.
[53] H. Pan, L. Liu, Z. X. Guo, L. Dai, F. Zhang, D. Zhu, R. Czerw, D. L. Carroll, *Nano. Lett.* **2003**, *3*, 29.
[54] M. Burghard, G. Duesberg, G. Philipp, J. Muster, S. Roth, *Adv. Mater.* **1998**, *10*, 584.
[55] J. Liu, M. J. Casavant, M. Cox, D. A. Walters, P. Boul, W. Lu, A. J. Rimberg, K. A. Smith, D. T. Colbert, R. E. Smalley, *Chem. Phys. Lett.* **1999**, *303*, 125.
[56] Q. Chen, L. Dai, *Appl. Phys. Lett.* **2000**, *76*, 2719.
[57] S. C. Tsang, Y. K. Chen, P. J. F. Harris, M. L. H. Green, *Nature* **1994**, *372*, 159.
[58] S. Huang, L. Dai, A. W. H. Mau, *J. Phys. Chem. B* **1999**, *103*, 4223.
[59] H. Shimoda, S. J. Oh, H. Z. Geng, R. J. Walker, X. B Zhang, L. E. McNeil, O. Zhou, *Adv. Mater.* **2002**, *14*, 899.
[60] A. M. Cassell, N. R. Franklin, T. W. Tombler, E. M. Chan, J. Han, H. Dai, *J. Am. Chem. Soc.* **1999**, *121*, 7975.
[61] E. Joselevich, C. M. Lieber, *Nano. Lett.* **2002**, *2*, 1137.
[62] B. Q. Wei, R. Vajtai, Z. J. Zhang, G. Ramanath, P. M. Ajayan, *J. Nanosci. Nanotech.* **2001**, *1*, 35.
[63] See, for example: a) M. Nath, B. C. Satishkumar, A. Govindaraj, C. P. Vinod, C. N. R. Rao, *Chem. Phys. Lett.* **2000**, *322*, 333; b) H. Ago, S. Ohshima, K. Uchida, T. Komatsu, M. Yumura, *Physica B* **2002**, *323*, 306.
[64] J. Li, C. Papadopoulos, J. M. Xu, *Appl. Phys. Lett.* **1999**, *75*, 367.
[65] T. Iwasaki, T. Motoi, T. Den, *Appl. Phys. Lett.* **1999**, *75*, 2044.
[66] W. Z. Li, S. S. Xie, L. X. Qian, B. H. Chang, B. S. Zou, W. Y. Zhou, R. A. Zhao, G. Wang, *Science* **1996**, *274*, 1701.
[67] J. Li, C. Papadopoulos, J. M. Xu, *Appl. Phys. Lett.* **1999**, *75*, 367.
[68] T. Kyotani, B. K. Pradhan, A. Tomita, *Bull. Chem. Soc. Jap.* **1999**, *72*, 1957.
[69] G. Che, B. B. Lakshmi, C. R. Martin, E. R. Fisher, R. S. Ruoff, *Chem. Mater.* **1998**, *10*, 260.
[70] J. Li, C. Papadopoulos, J. M. Xu, *Nature* **1999**, *402*, 253.
[71] W. Z. Li, J. G. Wen, Z. F. Ren, *Appl. Phys. Lett.* **2001**, *79*, 1879.
[72] C. N. R. Rao, R. Sen, B. C. Satishkumar, A. Govindaraj, *Chem. Commun.* **1998**, *1525*.
[73] Z. F. Ren, Z. P. Huang, J. H. Xu, P. B. Wang, M. P. Siegal, P. N. Provencio, *Science* **1998**, *282*, 1105.
[74] Z. P. Huang, J. W. Xu, Z. F. Ren, J. H. Wang, M. P. Siegal, P. N. Provencio, *Appl. Phys. Lett.* **1998**, *73*, 3845.
[75] K. Iwata, K. Takahashi, Y. Fujimoto, F. Okuyama, H. Sugie, V. Filip, *J. Appl. Phys.* **2001**, *90*, 3.
[76] Y. Hayashi, T. Otoguro, M. Kawana, H. Hayashi, S. Nishino, *ICPIG Proceedings 25th*, Nagoya, Japan. **2001**, *July*, 17 – 22.
[77] Y. H. Wang, J. Lin, C. H. A. Huan, G. S. Chen, *Appl. Phys. Lett.* **2001**, *79*, 5.
[78] H. Murakami, M. Hirakawa, C. Tanaka, H. Yamakawa, *Appl. Phys. Lett.* **2000**, *79*, 1776.
[79] S. H. Tsai, C. T. Shiu, S. H. Lai, L. H. Chan, W. J. Hsieh, H. C. Shih, *J. Mater. Sci. Lett.* **2002**, *21*, 21.
[80] L. J. Young, B. S. Lee, *Thin Film Solids* **2002**, *418*, 85.
[81] C. A. Bower, S. Jin, W. Zhu, *Eur. Pat. Appl.* **2001**, 18.
[82] Y. Avigal, R. Kalish, *App. Phys. Lett.* **2001**, *78*, 16.
[83] R. Kamalakaran, M. Terrones, T. Seeger, Ph. Kohler-Redlich, M. Ruhle, Y. A. Kim, T. Hayashi, M. Endo, *Appl. Phys. Lett.* **2000**, *77*, 21.
[84] S. Fan, M. G. Chapline, N. R. Franklin, T. W. Tomber, A. M. Cassell, H. Dai, *Science* **1999**, *283*, 512.
[85] J. Li, C. Papadopoulos, J. M. Xu, *Appl. Phys. Lett.* **1999**, *75*, 367.
[86] Z. F. Ren, Z. P. Huang, D. Z. Wang, J. G. Wen, J. W. Xu, J. H. Wang, L. E. Calvet, J. Chen, J. F. Klemic, M. A. Reed, *Appl. Phys. Lett.* **1999**, *75*, 1086.
[87] X. Wang, Y. Liu, D. Zhu, *Adv. Mater.* **2002**, *14*, 165, and references therein.
[88] D. C. Li, L. Dai, S. Huang, A. W. H. Mau, Z. L. Wang, *Chem. Phys. Lett.* **2000**, *316*, 349.
[89] Z. Liu, Z. Shen, T. Zhu, S. Hou, L. Ying, Z. Shi, Z. Gu, *Langmuir* **2000**, *16*, 3569.
[90] B. Wu, J. Zhang, Z. Wei, S. Cai, Z. Liu, *J. Phys. Chem. B* **2001**, *105*, 5075.
[91] X. Nan, Z. Gu, Z. Liu, *J. Col. Inter. Sci.* **2002**, *24*, 311.
[92] Y. Yang, S. Huang, H. He, A. W. H. Mau, L. Dai, *J. Am. Chem. Soc.* **1999**, *121*, 10832.
[93] J. March, *Advanced Organic Chemistry*, 4th ed., John Wiley, New York, **1992**.
[94] M. J. Bowden, *Adv. Chem. Ser.* **1988**, *218*, 1.
[95] Q. Chen, L. Dai, *J. Nanosci. Nanotechnol.* **2001**, *1*, 43.
[96] S. Huang, A. W. H. Mau, T. W. Turney, P. A. White, L. Dai, *J. Phys. Chem. B* **2000**, 104, 2193.
[97] H. Kind, J. M. Bonard, C. Emmenegger, L. O. Nilsson, K. Hernadi, E. Maillard-Schaller, L. Schlapbach, L. Forro, K. Kern, *Adv. Mater.* **1999**, *11*, 1285.
[98] R. J. Jackman, G. M. Whitesides, *Chemtech* **1999**, *May*, 18.
[99] Y. Xia, G. M. Whitesides, *Angew. Chem.* **1998**, *110*, 568; *Angew. Chem. Int. Ed.* **1998**, *37*, 550.
[100] L. Dai, H. J. Griesser, A. W. H. Mau, *J. Phys. Chem. B* **1997**, *101*, 9548.
[101] *Techniques & Applications of Plasma Chemistry* (Eds.: J. R. Hollan, A. T. Bell), Wiley, New York, **1974**.
[102] G. Zheng, H. Zhu, Q. Luo, Y. Zhou, D. Zhao, *Chem. Mater.* **2001**, *13*, 2240.
[103] J. I. Sohn, S. Lee, Y. Song, S. Choi, K. Cho, K. Nam, *Appl. Phys. Lett.* **2001**, *78*, 901.
[104] J. I. Sohn, C. Choi, S. Lee, T. Seong, *Appl. Phys. Lett.* **2001**, *78*, 3130.
[105] J. G. Wen, Z. P. Huang, D. Z. Wang, J. H. Chen, S. X. Yang, Z. F. Ren, J. H. Wang, J. H. Wang, L. E. Calvet, J. Chen, J. F. Klemic, M. A. Reed, *J. Mater. Res.* **2001**, *16*, 3246.
[106] K. B. K. Teo, M. Chhowalla, G. A. I. Amaratunga, W. I. Milne, D. G. Hasko, G. Pirio, P. Legagneux, F. Wyczisk, D. Pribat, *Appl. Phys. Lett.* **2001**, *79*, 1534.

[107] Z. J. Zhang, B. Q. Wei, G. Ramanath, P. M. Ajayan, *Appl. Phys. Lett.* **2000**, *77*, 23.
[108] B. Q. Wei, R. Vajtai, Y. Jung, J. Ward, R. Zhang, G. Ramanath, P. M. Ajayan, *Nature* **2002**, *416*, 495.
[109] R. Dagani, *Chem. Eng. News* **2002**, *April 8*, 11.
[110] S. Huang, L. Dai, *J. Phys. Chem. B* **2002**, *106*, 3543.
[111] X. Gong, L. Dai, H. J. Griesser, A. W. H. Mau, *J. Polym. Sci., Part B: Polym. Phys.* **2000**, *38*, 2323.
[112] Q. Chen, L. Dai, M. Gao, S. Huang, A. W. H. Mau, *J. Phys. Chem. B* **2001**, *105*, 618.
[113] L. Dai, H. A. W. St John, J. Bi, P. Zientek, R. C. Chatelier, H. J. Griesser, *Surf. Interface Anal.* **2000**, *29*, 46.
[114] M. Gao, S. Huang, L. Dai, G. Wallace, R. Gao, Z. Wang, *Angew. Chem.* **2000**, *112*, 3810; *Angew. Chem. Int. Ed.* **2000**, *39*, 3664.
[115] P. Poncharal, Z. L. Wang, D. Ugarte, W. A. de Heer, *Science* **1999**, *283*, 1513.
[116] R. Gao, Z. L. Wang, Z. Bai, W. A. de Heer, L. Dai, M. Gao, *Phys. Rev. Lett.* **2000**, *85*, 622.
[117] T. W. Odom, J. L. Huang, P. Kim, C. M. Lieber, *J. Phys. Chem. B* **2000**, *104*, 2794, and references therein.
[118] L. Dai, *J. Macromol. Sci., Rev. Macromol. Chem. Phys.* **1999**, *39*, 237, and references therein.
[119] L. Dai, A. W. H. Mau, *J. Phys. Chem. B* **2000**, *104*, 1891.
[120] C. V. Nguyen, L. Delzeit, A. M. Cassell, J. Li, J. Han, M. Meyyappan, *Nano Lett.* **2002**, *2*, 1079.
[121] Y. Miyamoto, A. Rubio, M. L. Cohen, S. G. Louie, *Phys. Rev. B* **1994**, *50*, 4976.
[122] Z. Weng-Sieh, K. Cherrey, N. G. Chopra, G. Nasreen, X. Blasé, Y. Miyamoto, A. Rubio, M. L. Cohen, S. G. Louie, A. Zettl, R. Gronsky, *Phys. Rev. B* **1995**, *51*, 1229.
[123] A. Zettl, *Adv. Mater.* **1996**, *8*, 443.
[124] W. Q. Han, J. Cumings, X. Huang, K. Bradley, A. Zettl, *Chem. Phys. Lett.* **2001**, *346*, 368.
[125] D. Gong, C. A. Grimes, O. K. Varghese, W. Hu, R. S. Singh, Z. Chen, E. C. Dickey, *J. Mater. Res.* **2001**, *16*, 3331.
[126] J. Bao, C. Tie, Z. Xu, Q. Zhou, D. Shen, Q. Ma, *Adv. Mater.* **2001**, *13*, 1631.
[127] A. Michailowski, D. Almawlawi, G. Cheng, M. Moskovits, *Chem. Phys. Lett.* **2001**, *349*, 1.
[128] a) K. B. Shelimov, D. N. Davydov, M. Moskovits, *Appl. Phys. Lett.* **2000**, *77*, 1722; b) K. B. Shelimov, M. Moskovits, *Chem. Mater.* **2000**, *12*, 250.
[129] a) F. L. Deepak, C. P. Vinod, K. Mukhopadhyay, A. Govindaraj, C. N. R. Rao, *Chem. Phys. Lett.* **2002**, *353*, 345; b) D. Golberg, Y. Bando, M. Mitome, K. Kurashima, T. Sato, N. Grobert, M. Reyes-Reyes, H. Terrones, M. Terrones, *Physica B* **2002**, *323*, 60.
[130] R. C. Smith, W. M. Fischer, D. L. Gin, *J. Am. Chem. Soc.* **1997**, *119*, 4092.
[131] M. Fu, Y. Zhu, R. Tan, G. Shi, *Adv. Mater.* **2001**, *13*, 1874.
[132] C. R. Martin, *Acc. Chem. Res.* **1995**, *28*, 61.
[133] C. G. Wu, T. Bein, *Science* **1994**, *266*, 1013.
[134] V. M. Cepak, C. R. Martin, *Chem. Mater.* **1999**, *11*, 1363.
[135] a) C. R. Martin, *Adv. Mater.* **1991**, *3*, 457; b) C. R. Martin, *Adv. Mater.* **1991**, *3*, 457.
[136] R. V. Parthasarathy, C. R. Martin, *Chem. Mater.* **1994**, *6*, 1627.
[137] a) M. Steinhart, J. H. Wendorff, A. Greiner, R. B. Wehrspohn, K. Nielsch, J. Schilling, J. Choi, U. Gösele, *Science* **2002**, *296*, 1997; b) M. Steinhart, J. H. Wendorff, R. B. Wehrspohn, *ChemPhysChem* **2003**, *4*, 1171.
[138] T. Kyotani, T. Nagai, S. Inoue, A. Tomita, *Chem. Mater.* **1997**, *9*, 609.
[139] R. V. Parthasarathy, K. L. N. Phani, C. R. Martin, *Adv. Mater.* **1995**, *7*, 896.
[140] H. Qiu, M. Wan, B. Matthews, L. Dai, *Macromolecules* **2001**, *34*, 675.
[141] M. X. Wan, J. C. Li, *J. Polym. Sci., Part A: Polym. Chem.* **1999**, *37*, 4605.
[142] L. T. Qu, G. Q. Shi, F. Chen, J. X. Zhang, *Macromolecules* **2003**, *36*, 1063.
[143] S. Fernandez-Lopez, S. H. Kim, E. C. Choi, M. Delgado, J. R. Granja, A. Khasanov, K. Kraehenbuehl, G. Long, D. A. Weinberger, K. M. Wilcoxen, M. R. Ghadiri, *Nature* **2001**, *412*, 452.
[144] A. M. Rouhi, *Chem. Eng. News* **2001**, *79*, 41.

Received: April 2, 2003 [A 770]

